NAVAL POSTGRADUATE SCHOOL

MONTEREY, CALIFORNIA

THESIS

INVESTIGATION OF TRANSIENT PLASMA IGNITION FOR A PULSE DETONATION ENGINE

by

Joel Rodriguez

March 2005

Thesis Advisor:	Jose O. Sinibaldi
Second Reader:	Christopher M. Brophy

THIS PAGE INTENTIONALLY LEFT BLANK

REPORT DOCUMENTATION PAGE			Form Approved OMB No. 0704-0188
Public reporting burden for this collection of information is estimated to average 1 hour per response, including the time for reviewing instruction, searching existing data sources, gathering and maintaining the data needed, and completing and reviewing the collection of information. Send comments regarding this burden estimate or any other aspect of this collection of information, including suggestions for reducing this burden, to Washington headquarters Services, Directorate for Information Operations and Reports, 1215 Jefferson Davis Highway, Suite 1204, Arlington, VA 22202-4302, and to the Office of Management and Budget, Paperwork Reduction Project (0704-0188) Washington DC 20503.			
1. AGENCY USE ONLY ***(Leave blank)***	**2. REPORT DATE** March 2005	**3. REPORT TYPE AND DATES COVERED** Master's Thesis	
4. TITLE AND SUBTITLE: Investigation of Transient Plasma Ignition for a Pulse Detonation Engine			**5. FUNDING NUMBERS**
6. AUTHOR(S) Joel Rodriguez			
7. PERFORMING ORGANIZATION NAME(S) AND ADDRESS(ES) Naval Postgraduate School Monterey, CA 93943-5000			**8. PERFORMING ORGANIZATION REPORT NUMBER**
9. SPONSORING /MONITORING AGENCY NAME(S) AND ADDRESS(ES) Office of Naval Research (ONR) Ballstone Tower One 800 N. Quincy St. Arlington, VA 22217-5660			**10. SPONSORING/MONITORING AGENCY REPORT NUMBER**
11. SUPPLEMENTARY NOTES The views expressed in this thesis are those of the author and do not reflect the official policy or position of the Department of Defense or the U.S. Government.			
12a. DISTRIBUTION / AVAILABILITY STATEMENT Approved for public release; distribution is unlimited			**12b. DISTRIBUTION CODE**

13. ABSTRACT (maximum 200 words)

Elimination or reduction of auxiliary oxygen use in Pulse Detonation Engines (PDEs) is necessary if the technology is to compete with existing Ramjet systems. This thesis investigated a Transient Plasma Ignition (TPI) system and found that the technology can at least reduce and may be able to completely remove the auxiliary oxygen requirement of current PDE systems. TPI was tested and compared with a traditional capacitive discharge spark plug system in a dynamic flow, ethylene/air mixture combustor. Ignition delay time, Deflagration-to-Detonation transition (DDT) distance and time, detonation wave speed and fire success rate performance were analyzed for various mass flow rates and stoichiometric ratios. A transient plasma dual-electrode concept was also employed and analyzed.

Results show that TPI is more effective and reliable than the spark plug ignition with considerable improvements to DDT performance. The TPI dual-electrode concept was proven to be the most effective configuration with average reductions in DDT distance and time of 17% and 41% respectively when compared to the capacitive discharge spark plug system configuration.

14. SUBJECT TERMS Pulse Detonation Engines, PDE, PDE Ignition, Transient Plasma Ignition, Pseudo-spark Discharge			**15. NUMBER OF PAGES** 79
			16. PRICE CODE
17. SECURITY CLASSIFICATION OF REPORT Unclassified	**18. SECURITY CLASSIFICATION OF THIS PAGE** Unclassified	**19. SECURITY CLASSIFICATION OF ABSTRACT** Unclassified	**20. LIMITATION OF ABSTRACT** UL

NSN 7540-01-280-5500 Standard Form 298 (Rev. 2-89)
Prescribed by ANSI Std. 239-18

THIS PAGE INTENTIONALLY LEFT BLANK

Approved for public release; distribution is unlimited

INVESTIGATION OF TRANSIENT PLASMA IGNITION FOR A PULSE DETONATION ENGINE

Joel Rodriguez
Lieutenant, United States Navy
B.S., United States Naval Academy, 1998

Submitted in partial fulfillment of the
requirements for the degree of

MASTER OF SCIENCE IN ASTRONAUTICAL ENGINEERING

from the

NAVAL POSTGRADUATE SCHOOL
March 2005

Author: Joel Rodriguez

Approved by: Jose O. Sinibaldi
Thesis Advisor

Christopher M. Brophy
Second Reader

Anthony J. Healey
Chairman, Department of Mechanical & Astronautical Engineering

THIS PAGE INTENTIONALLY LEFT BLANK

ABSTRACT

Elimination or reduction of auxiliary oxygen use in Pulse Detonation Engines (PDEs) is necessary if the technology is to compete with existing Ramjet systems. This thesis investigated a Transient Plasma Ignition (TPI) system and found that the technology can at least reduce and may be able to completely remove the auxiliary oxygen requirement of current PDE systems. TPI was tested and compared with a traditional capacitive discharge spark plug system in a dynamic flow, ethylene/air mixture combustor. Ignition delay time, Deflagration-to-Detonation transition (DDT) distance and time, detonation wave speed and fire success rate performance were analyzed for various mass flow rates and stoichiometric ratios. A transient plasma dual-electrode concept was also employed and analyzed.

Results show that TPI is more effective and reliable than the spark plug ignition with considerable improvements to DDT performance. The TPI dual-electrode concept was proven to be the most effective configuration with average reductions in DDT distance and time of 17% and 41% respectively when compared to the capacitive discharge spark plug system configuration.

THIS PAGE INTENTIONALLY LEFT BLANK

TABLE OF CONTENTS

THIS PAGE INTENTIONALLY LEFT BLANK

LIST OF FIGURES

LIST OF TABLES

THIS PAGE INTENTIONALLY LEFT BLANK

ACKNOWLEDGMENTS

The author wishes to recognize and express his appreciation and admiration to Professors Sinibaldi and Brophy for their enthusiasm, encouragement, and patient assistance throughout this thesis work; many thanks also go to Mr. George Hageman for his extraordinary dedication and technical expertise.

The efforts and support of our colleagues at the University of Southern California (USC) and our sponsors at the Office of Naval Research (ONR) are acknowledged and truly appreciated.

For God and Country.

THIS PAGE INTENTIONALLY LEFT BLANK

I. INTRODUCTION

This chapter introduces Pulse Detonation Engines. The history and overall progress made with the technology is discussed in section A. Theory of detonations and the Deflagration to Detonation Transition process is discussed in the following section. Section C features PDE thermodynamics and operation cycle. Finally, PDE ignition technology is described and the motivation for this thesis is discussed.

A. HISTORICAL BACKGROUND

Pulse Detonation Engines (PDEs) are descendants of the pulse jet propulsion plants that powered the German V-1 flying bomb during World War II. Unlike the pulse jet, PDEs detonate rather than deflagrate their propellants. Over the past 6 decades, there have been numerous theoretical and experimental efforts aimed at understanding and harnessing detonations in propulsion and other applications [1].

The groundwork for the PDE concept was laid by the pioneering work of Hoffman in the 1940's. Hoffman achieved detonations with acetylene and benzene and liquid oxygen [2]. Circa 1957, Nicholls [3] conducted single and multi-cycle studies with hydrogen and acetylene fuels, and oxygen and air oxidizers. In 1962, Krzycki [4] achieved 60 Hertz (Hz) operation but failed to detonate propane air mixtures in an experimental setup similar to Nicholls'. It was not until later, in 1986, that more multi-cycle research work took place and detailed results were reported by Helman and Smirnov [5]. Smirnov employed gasoline-air mixtures while Helman employed ethylene/oxygen and ethylene/air mixtures.

With the maturation of Computational Fluid Dynamics (CFD) in the late 1980's, PDEs started to be modeled computationally. Cambier and Adelman (1988) [6] and Eidelman (circa 1990), computationally analyzed the performance of PDE devices [7]. The 1990's saw a renaissance in PDE experimentation with multiple efforts involving industry, academia and the military. In 1999, the Office of Naval Research (ONR), brought Pratt & Whitney, Boeing, and several academic institutions (including the Naval Postgraduate School) together to work on the Pulse Detonation Engine Risk Reduction

program. ONR's goal is to contribute to overall PDE technology advancement and aims to develop a pure fuel/air PDE for a Mach 2-4, long range stand-off weapon and apply PDE technology expertise to potential unmanned air vehicles (UCAVs) and underwater propulsion applications [8].

Currently, there are several PDE research programs sponsored by the U.S. Air Force, NASA, Defense Advanced Research Project Agency and ONR among others internationally. General Electric (GE), Pratt & Whitney and Rolls Royce are earnestly pursuing PDE technology as the improvements of gas turbine technology have begun to reach the limits of fuel efficiency and thrust to weight ratios. Pratt & Whitney has even begun to apply PDE technology to non-propulsion engineering problems with its Ash and Slag Detonation Online Cleaning System. The derivative innovation removes slag and ash from utility coal boilers [9]. When PDE technology reaches the current maturity of gas turbines and ramjets, one may see a new breed of efficient supersonic airliners, spacecraft launch vehicles, lunar and planetary landers, and excursion vehicles.

B. THEORY OF DETONATIONS

1. Detonation Wave Theory

Figure 1 helps to visualize what occurs in physical terms following the motion of a detonation wave through a flammable mixture. Chapman (1899) and Jouguet (1905, 1906) experimentally observed detonation waves and presented the first theory of a detonation combustion wave [10]. Chapman and Jouguet (CJ) solved conservation of mass, momentum and energy equations one-dimensionally obtaining two significant results. First, the steady state value for the detonation wave velocity, named CJ-velocity after them. Secondly, the thermodynamic conditions of combustion products immediately behind the detonation wave. This special thermodynamic state is known as the CJ condition. Using CJ theory, one may determine detonation velocity and combustion product conditions for a known mixture [10].

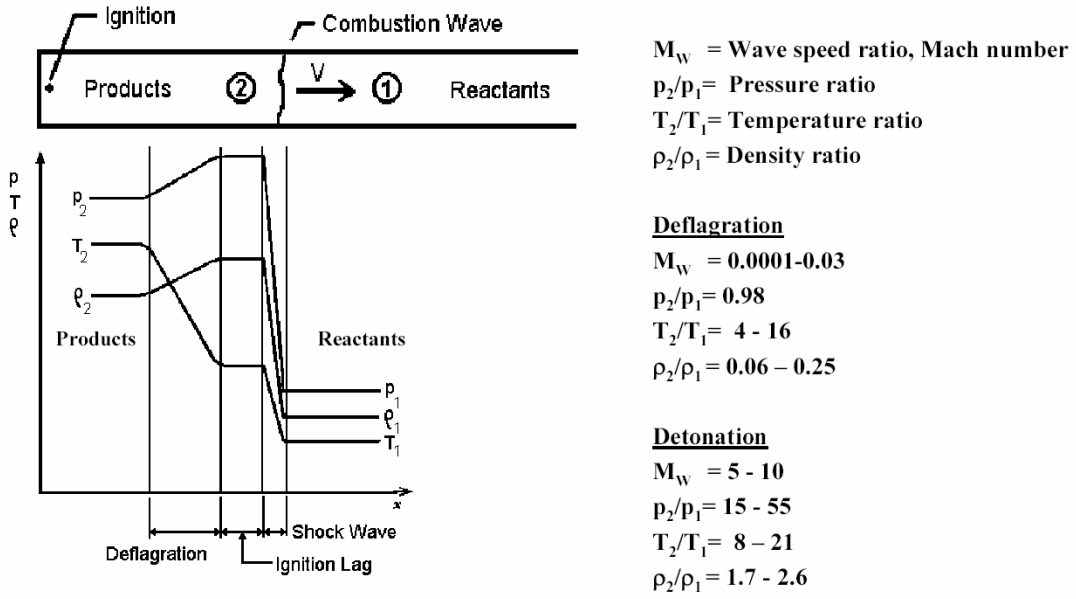

Figure 1. Physical Property Differences across Deflagration and Detonation waves in Gases (after Ref. [11])

In the 1940's, Zeldovich, von Neumann and Doring improved the CJ theory model by incorporating chemical induction time in similar models [12]. The ZND models yields the same detonation velocities and pressures results as the CJ-theory. The only fundamental difference between the two models is the thickness of the wave [10]; where as the CJ-model assumes and infinitesimal wave thickness, the ZND model calculate a finite wave thickness. Wave structure is in reality three-dimensional and much more complex than modeled by the CJ and ZND models. The evolution from one-dimensional detonation wave structure to multi-dimensional wave structure analysis can be found in several comprehensive papers by Oppenheim, Manson, and Wagner, Strehlow, Lee, Soloukhin, and Oppenheim, Schott, Schelkin, and van Tiggelen and de Soete [11]. Wave structure characteristics are significant for wave behavior analysis and PDE design geometry.

A propagating detonation wave has a complex three-dimensional cellular structure characterized by a leading, non-planar shock wave made up at every instant of curved Mach-stem, incident and reflected shocks. Convex toward the incoming flow, the shocks intersect at a point termed as the triple point. Soot tracks of a hydrogen/oxygen

and 70% argon mixture detonation is shown in Figure 2. The tracks reveal the wave structure and the presence of the triple points at intersecting triple shock waves. The characteristic cell size of the wave structure is defined as λ. Cell size is mixture-dependent and is a critical parameter for detonation. Past PDE research has determined a critical combustor tube diameter required for successful detonation transmission into an infinite volume. The critical tube diameter has been determined to be 13 times the cell size, 13λ, for most practical propulsion mixtures. Mixtures with highly regular cell structures may require larger tube diameter than 13λ [13].

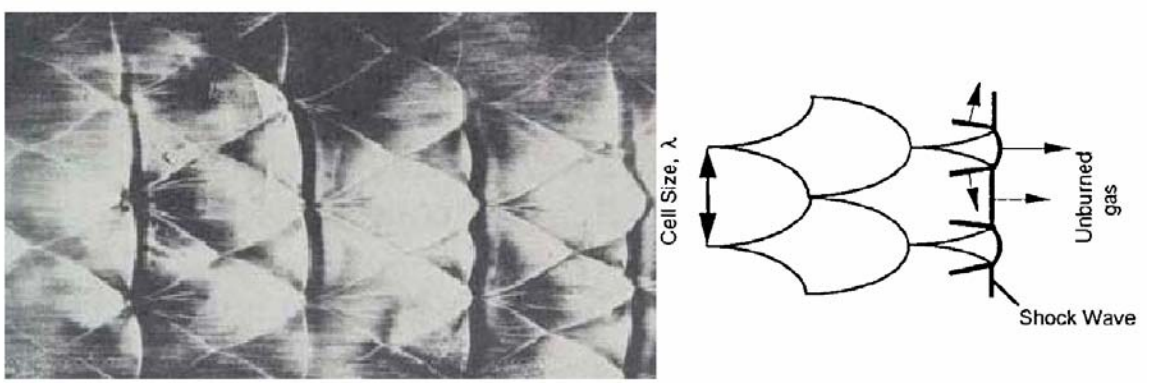

Figure 2. Soot track of a Detonation Wave and Structure Schematic (after Refs. [11] and [10])

2. Deflagration to Detonation Transition (DDT)

Deflagration to Detonation transition (DDT) is the process by which a laminar flame changes propagation mechanisms and eventually develops into of a self-sustaining detonation wave. DDT is a complex phenomenon. It is essential for PDE researchers to understand and control DDT in PDE designs [14]. DDT can be summarized as follows: (1) Ignition and wave propagation. (2) Flame wrinkling, turbulence onset and dramatic increase in burning rate. (3) Increased burning rates increase flow velocity ahead of the mixture due to expanding gases. Unsteady compression waves ahead of flame front increase temperature sufficiently to produce an acceleration effect on reaction rates. Shock front formation occurs due to coalescence of compression waves. (4) Detonation onset, “explosion in an explosion”, where there is an abrupt appearance of explosion centers or “hot spots” in the shock. (5) The detonation wave propagates, if successful,

developing into a pseudo-steady, self-sustaining wave at a CJ wave speed and thermodynamic conditions [7].

The DDT process can be aided by the employment of obstacles in the flow path of a PDE combustor tube. Comprehensive research at McGill University, determined an obstacle blockage ratio of 0.4 and spacing of approximately 1 tube diameter as the near optimum for length scale improvement for DDT in terms of obstacle blockage and spacing. DDT does occur in smooth combustor tubes but the length required for DDT to occur, DDT distance, may be an order of magnitude larger [14]. Minimization of DDT distance and DDT time is essential for a production PDE's mass and operational frequency. Therefore event (3) in Figure 4 is our prime candidate to optimize.

Figure 3 provides an elegant illustration of the DDT process. From the work of Urtiew and Oppenheim, the illustration shows a stroboscopic Schlieren record of DDT in $2H_2$+ O_2 mixture at a pressure of 554 Torr. Twenty one images are presented, one every 5 microseconds as indicated in the figure's vertical axis. Distance in meters is annotated in the figure's horizontal axis. A pressure trace, an instrumental for PDE researchers, is inserted at the figure's upper right and describes the pressure history at labeled points 1 and 2 (top). In the insert, 1 division equals 200 pounds per square inch (psi) in the vertical scale and 50 microseconds in the horizontal scale. The insert's oscilloscope sweep leads the photographs by 180 microseconds. From Figure 7 and its pressure trace insert, one can estimate from the data that the DDT length in the given case was 0.29 meters, DDT time was approximately 90 microseconds and with a wave velocity of 3030 meters per second.

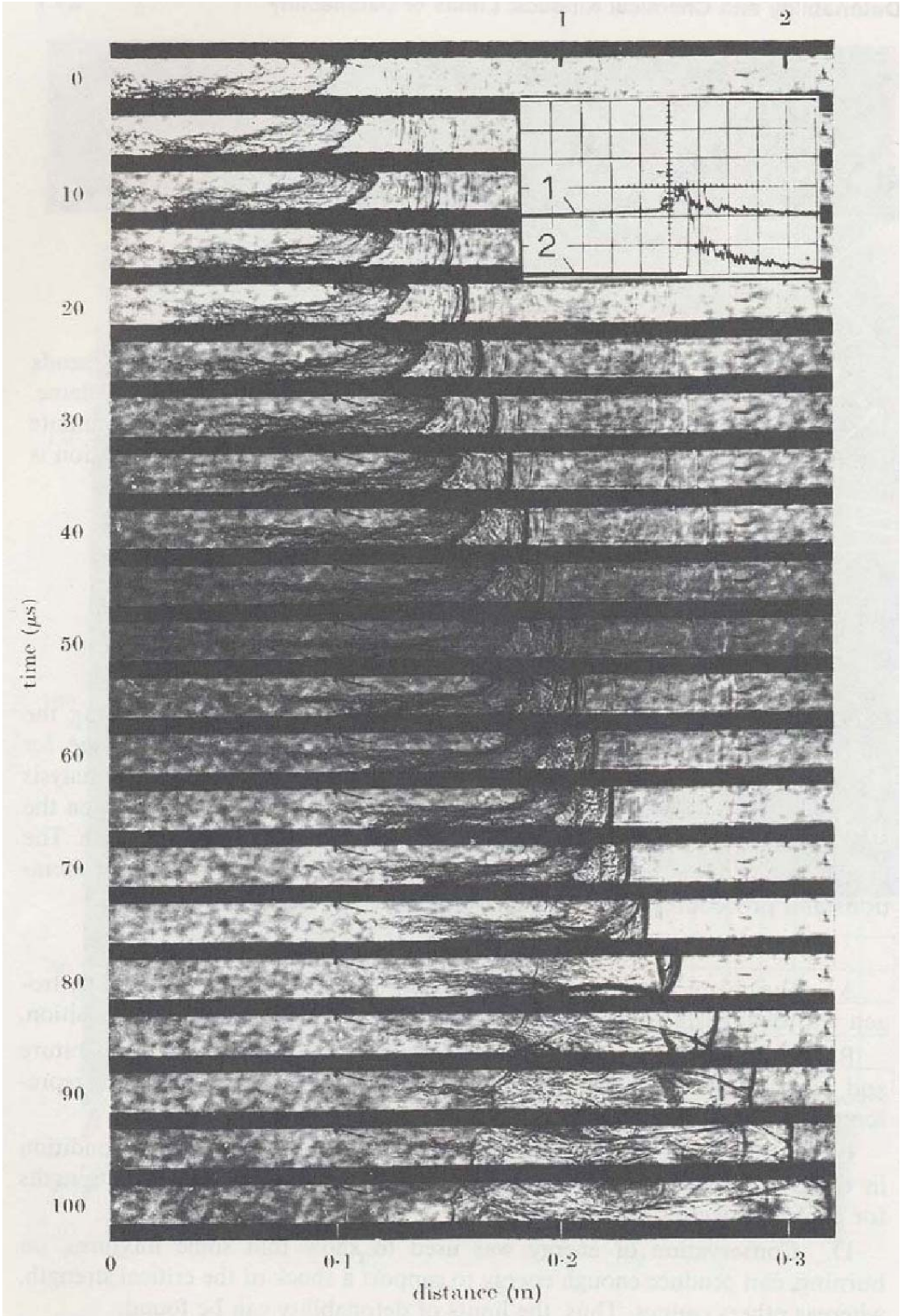

Figure 3. Schlieren Record of Deflagration- to- Detonation Transition (DDT) (from Ref. [11])

C. PDE THERMODYNAMICS AND OPERATION

1. Thermodynamic Cycle of a PDE

Using Figure 4 as reference, in a typical PDE, a fuel/oxidizer mixture will be injected and ignited near the closed end or head end. If a successful transition from deflagration to detonation occurs, a detonation travels from the closed end to the open end leaving behind high pressure and high temperature products which generate thrust as they expand and exit. A PDE produces thrust by this periodic or cyclic detonation of the fuel/oxidizer mixture; ideally air alone will serve as oxidizer for an air-breathing propulsion system.

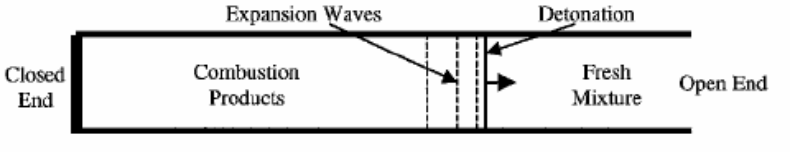

Figure 4. Schematic of a Simplified Pulse Detonation Engine (from Ref. [1])

Unlike in deflagration, where a laminar or turbulent flame front travels in the order of centimeters or meters per second, detonation wave fronts propagate at supersonic velocities in the order of 1.5 to 2 kilometers per second. The supersonic shock compresses and ignites the mixture almost instantaneously in a thin, high-pressure heat-release zone considered to be a constant volume process. Traditional air-breathing gas turbines, ramjets and rocket engines rely on constant pressure (isobaric) deflagration combustion. Therefore, a thermodynamic analysis comparison is useful and feasible [7].

The Brayton thermodynamic cycle is used for constant pressure process analysis and the Humphrey or Atkinson thermodynamic cycle is used for constant volume process analysis. Figure 5 illustrates the pressure, volume, temperature and entropy of both cycles. The cycles transfer work to and from the system by isentropic (constant entropy) compression and expansion. However, heat addition in the Brayton cycle, steps 2-5, is replaced by Humphrey's steps 2-3, occurring at constant volume.

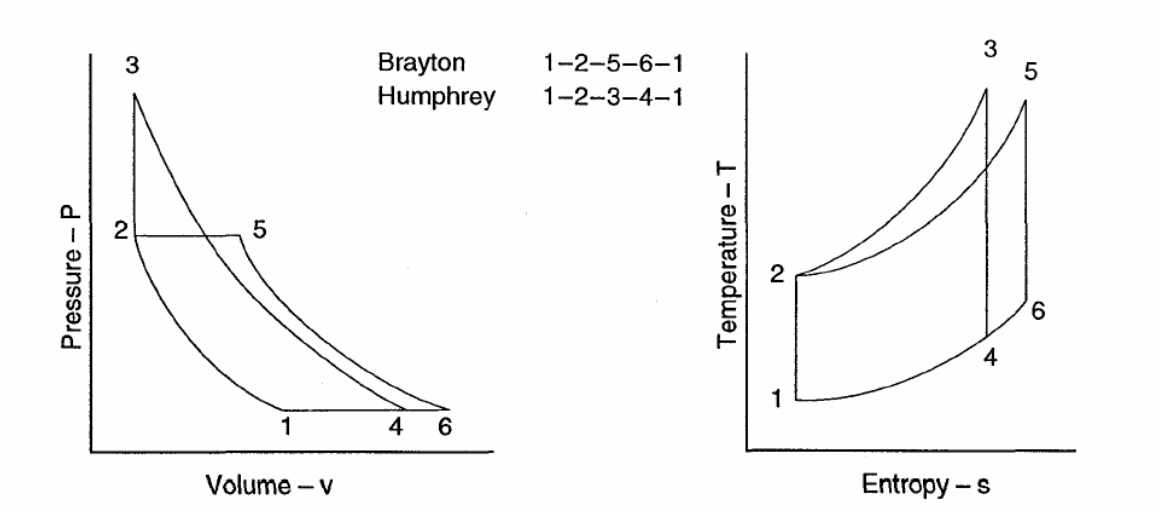

Figure 5. Pressure vs. Volume and Temperature vs. Entropy relationships between constant pressure Brayton and constant volume Humphrey Cycles (from Ref. [7])

Cycle thermal efficiency can be defined as the total useful work output compared to the total energy input as shown in Equations 1 and 2:

$$\eta_{Brayton} = 1 - \frac{T_1}{T_2} \qquad (1)$$

$$\eta_{Humphrey} = 1 - \gamma\left(\frac{T_1}{T_2}\right)\left[\frac{\left(\frac{T_3}{T_2}\right)^{\frac{1}{\gamma}} - 1}{\left(\frac{T_3}{T_2}\right) - 1}\right] \qquad (2)$$

η = Thermal efficiency

T = Temperature

γ = Specific heat ratio

Based on a detonation of a stoichiometric hydrogen/oxygen mixture at standard atmospheric conditions, calculations yield a temperature ratio T_3/T_2 of 12.3 and specific heat ratios γ of 1.4 in reactants and 1.13 in burned products. Figure 6 shows the calculated cycle thermal efficiency for average cycle specific heat ratios of 1.4 and 1.13 as a function of the compression ratio at steps 1-2 (P_2/P_1). The thermal efficiency of the constant pressure Brayton cycle is also plotted for comparison. Thermodynamic

efficiency improvement is noted. For example, at a compression factor of 10, the detonation cycle would offer efficiencies improvement ranging from approximately 19 to 42% over the Brayton isobaric cycle. The actual improvement efficiency would lie in between the limits bounded by the specific heats. This theoretical efficiency improvement may be translated into a specific impulse performance measure improvement of how the efficiently the engine converts propellant into useful thrust keeping in mind that this is only an approximation of ideal cycles. Overall performance may be improved by the employment of nozzles at the end of the tube for thrust augmentation [7].

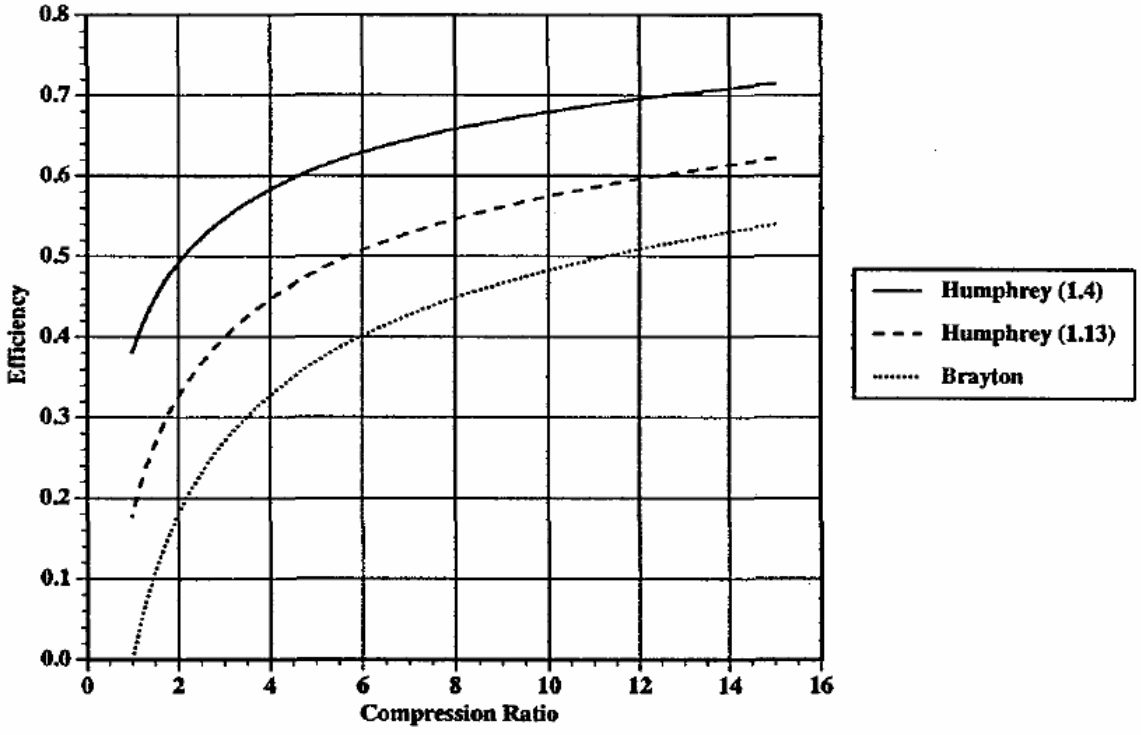

Figure 6. Thermal efficiency comparison of Humphrey detonation and Brayton cycles as a function of Compression Ratio (from Ref. [7])

Figure 7.

2. PDE Operating Cycle

The PDE operating cycle illustrates one of the devices attractive advantages, simplicity of design. Though fundamentally straightforward, the challenges presented by minuscule time scales and control requirements to achieve reliable multi-cycle operation are not entirely trivial but nevertheless achievable. The operational cycle of a typical PDE is shown in Figure 7. The cycle begins with propellants, fuel/oxidizer, mixture and

injection (1). The engine's combustor tube fills, purging previous combustion products if any (2). Event (3) shows mixture ignition. Events (4) and (5) show detonation wave formation and detonation wave exit. In event (7) a series of rarefaction waves begin to reduce the pressure inside the combustor tube and the combustion products are purged from the combustor tube, event (8). The cycle then repeats starting again with event (1).

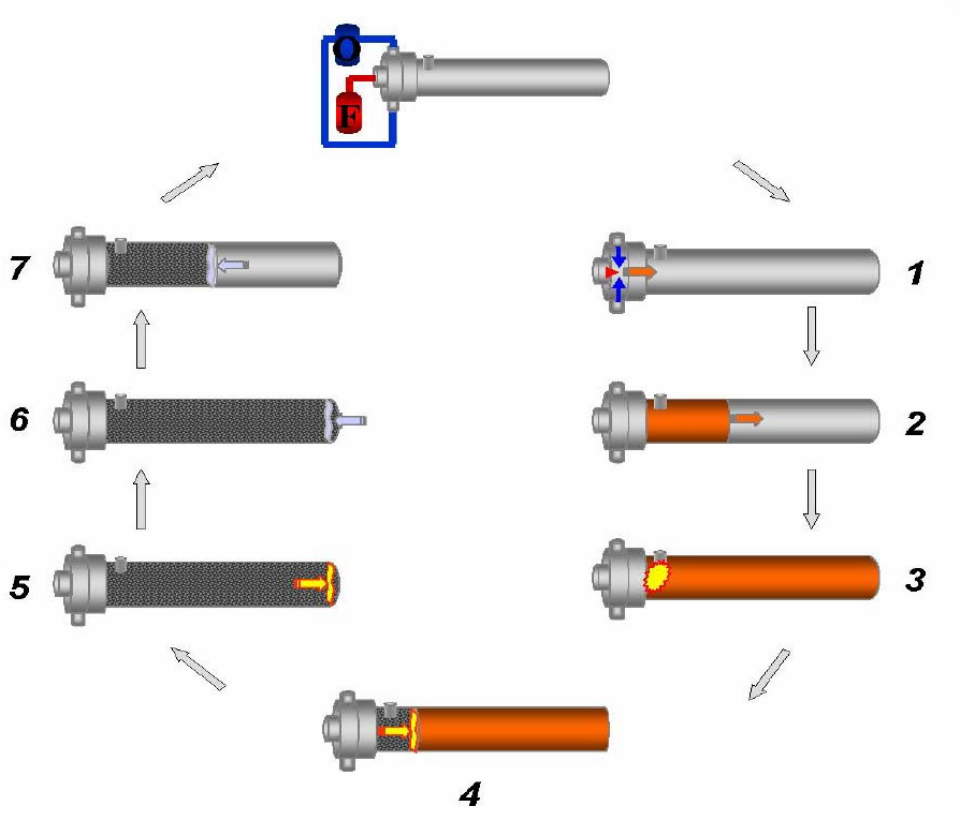

Figure 8. PDE Operating Cycle

The duration of a cycle on a typical PDE is on the order of tens of milliseconds. Events (4) and (5) occur in the microsecond scale. Experimental results up to date suggests that in order to achieve practical thrust levels, PDE operational frequencies greater than 60 Hz are required. Therefore, one must minimize the required time to execute each of the PDE cycle events. Events (4) and (5) are already on the order of 10 microseconds. Events (1), (2), (6), and (7) are gas dynamics-dominated events. Event (3) is dominated by combustion factors such as chemical reaction rates and turbulence intensity which enhances mixing.

D. PDE IGNITION TECHNOLOGY

Effective and reliable detonation initiation in fuel/air mixtures is one of the most important challenges in the development of a practical PDE. There are 3 different methods of initiating a wave. These methods are as follows: (1) Direct Initiation, (2) Deflagration to Detonation Transition, and (3) Shock-Induced Detonations. These methods are described below.

1. Direct Initiation Method

To directly initiate and detonation wave, a critical minimum energy deposition must occur in a very short time (compare to chemical kinetic reaction times). This process usually requires the use of an explosive charge to effectively deliver the large energies required. Another method that has had some success is to focus a set of high-powered pulsed laser beams into a point [20]. Neither of these methods is practical for a multi-cycle PDE. For instance, the use of explosive charges at PDE frequencies would create prohibitive mass requirements and complex explosive management issues.

2. DDT Method

Deflagration to Detonation transition (DDT) is the process by which a laminar flame changes propagation mechanisms and eventually develops into of a self-sustaining detonation wave. DDT can be summarized as follows: (1) Ignition and wave propagation. (2) Flame wrinkling, turbulence onset and dramatic increase in burning rate. (3) Increased burning rates increase flow velocity ahead of the mixture due to expanding gases. Unsteady compression waves ahead of flame front increase temperature sufficiently to produce an acceleration effect on reaction rates. Shock front formation occurs due to coalescence of compression waves. (4) Detonation onset, “explosion in an explosion”, where there is an abrupt appearance of explosion centers or “hot spots” in the shock. (5) The detonation wave propagates, if successful, developing into a pseudo-steady, self-sustaining wave at a CJ wave speed and thermodynamic conditions [7].

There is a significant and comprehensive database of research PDEs that employ this method of detonation initiation. This method uses low energies for ignition and has been employed with wide range of mixtures. Internal DDT obstacles are often required for achieve detonation within a short tube unless there is the use of auxiliaryor supplementary oxygen beyond the levels of that found in air. It is important to note that

the use of DDT obstacles has significant impact in PDE performance as it does inherently create drag losses and mass penalties.

3. Shock-Induced Detonation

In this method high pressure and temperature behind shock waves start the mechanical reaction in the mixture behind the shock wave and if critical pressure and temperature are reached behind the shock, a detonation wave is initiated. This method has been proven to be very effective in recent years. For PDEs, only the DDT method and the Shock-Induced Method or a combination of the two is practical.

Two shock-induced detonation techniques have been studied in significant detail: shock focusing and the initiator (pre-detonator) approach. In shock focusing, geometry is used to manipulate, collide or otherwise enhance shock or shocks in order to accomplish DDT. Extremely geometry dependent, hard to generate reliably and highly dynamic, shock focusing has achieved limited success.

A hybrid approach is where DDT is used in a fuel/oxygen mixture to produce a shock that in turn induces a detonation in a less sensitive mixture on a bigger main combustor. The concept of this detonation-to-detonation unit is to use a small tube (1% or less volume of the main combustor's volume) which is filled with highly sensitive mixture, such as ethylene/O_2 or JP-10/O_2 [15]. A detonation is rapidly created in the "initiator" and discharged into the main combustor where a less sensitive mixture awaits, such as ethylene/air or JP-10/air. Effective transmission is key for success and is defined as one in which the detonation wave exiting the smaller combustor overcomes the diffraction process and continues propagating into the less sensitive fuel-air mixture as a detonation wave. An effective transmission also results when a detonation wave exiting the initiator tube fails during the diffraction process while entering the main combustor due to the diffraction process weakening the leading shock, but due to reflection and/or shock focusing/reflection processes which may occur in the gas dynamic flow downstream of the initiator tube, a detonation re-initiation process occurs and thus an "effective" transmission occurs. The re-initiation process is therefore due to the production of local hot spots where detonation re-initiation occurs [16].

4. Transient Plasma Ignition (TPI)

Transient Plasma Ignition has been research for propulsion systems most recently. In TPI, a pseudo-spark (corona) discharge in the tens of nanoseconds time scale can be applied to a quiescent mixtures or dynamic mixture flow.

Corona discharges (the portion of an electric discharge before the onset of the low-voltage, high current arc discharge) are fundamentally plasmas that are in a transient, formative phase. These discharges have the potential to overcome many of the limitations of conventional electric as CD Spark discharges and laser discharges for reasons that include: (1) better coupling into gas because the cross-section for dissociation and ionization more nearly matches the electron energy distribution function; (2) lower losses through lower radiation, lower anode and cathode losses, and lower gas dynamic disturbance formation; (3) there are many streamers, each of which has a similar energy content, as opposed to a single, unnecessarily large and intense arc, which in turn can initiate combustion in a larger volume and (4) the size and shape of the ignition volume can be tailored using the geometry of the anode and cathode [17].

With recent advances in pulsed power electronics, such discharges can be produced efficiently in systems of reasonable cost, size and mass. Professor Martin Gundersen and his team at USC's Department of Electrical Engineering, Electrophysics Division, has developed energy-efficient transient plasma ignition systems appropriate for PDE research. Preliminary results have demonstrated that TPI reduced ignition delay by at least factor of 3 signaling significant promise in the use of the technology for improvements in ignition reliability, DDT and performance.

E. MOTIVATION

The motivation of this thesis is to evaluate TPI and determine if it can successfully remove the auxiliaryoxygen requirement in current PDE technology. As shown in Figure 8, the NPS valveless PDE design utilizes continuous airflow through the engine flow path and does not modulate the airflow through the use of valves as with most designs. The primary airflow to the engine is metered upstream of a vitiator through a choke with associated total pressure and temperature transducers. Fuel injection is controlled by four high-speed solenoid valves and therefore, the design is not truly "valveless" [15].

An oxygen-enriched initiator is used to induce a detonation in the main combustor. The initiator operates on an ethylene/oxygen/nitrogen mixture. During normal operation, the main combustor and initiator are charged simultaneously. When the respective mixtures in both sections reach their exit plane a MSD 6A CD Spark plug ignition system ignites the initiator. After a short DDT length in the initiator, a detonation forms and then transmits to the main combustor through a diffraction process.

Current experimental estimates for the specific impulse, $I_{sp,}$ performance of this PDE configuration show significant potential for PDE technology to become competitive with current Ramjet technology.

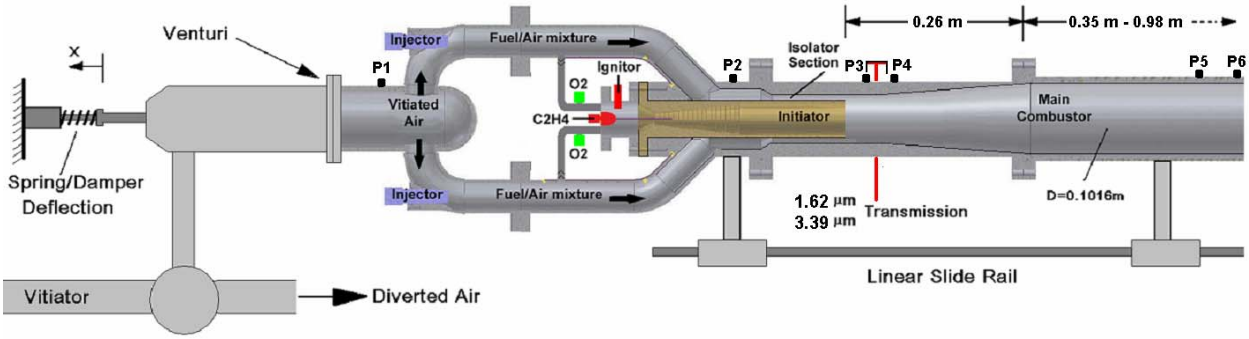

Figure 9. NPS Valveless PDE Design (from Ref. [15])

By analyzing Equation 3, one can surmise that specific impulse, $I_{sp,}$ performance improvement can be achieved by the reduction or elimination of the requirement of initiator auxiliary(supplementary) oxygen, $m_{O_2\ Aux}$, in the denominator . As:

$$I_{sp_f} = \frac{F}{m_{fuel} g} = \frac{F}{(m_{fuel} + m_{Initiator\ fuel} + m_{O_2\ Aux}) g} \qquad (3)$$

where:

I_{sp}= Specific impulse
g = Gravity acceleration constant
m = Mass
F = Force, thrust force
O = Oxygen
f = Fuel

Figure 9 presents an ideal comparison of specific impulse as a function of Mach number for PDE, ramjet and turbojet propulsion with an afterburner (AB) with compressor ratios of 30 (top plot) and 4 (middle turbojet plot) [18] . The results are from an experimentally validated, one-dimensional, time-accurate, reactive, computational fluid dynamics (CFD) Euler solver. The assumptions of the code are ideal but the code does model complex cycle gas-dynamics realistically. A complete description of this performance evaluation method and its results can be found in reference [18].

Compared with ramjet propulsion, the PDE shows significant advantages in Mach numbers below 3.5. Experimental specific impulse results from the NPS valveless design presented above range from 1500 to 1800 seconds at a simulated flight Mach number of 2.1, at a modest operating frequency of just 40 Hz with the undesired initiator oxygen performance penalty [15]. These experimental results are representative of ramjet performance.

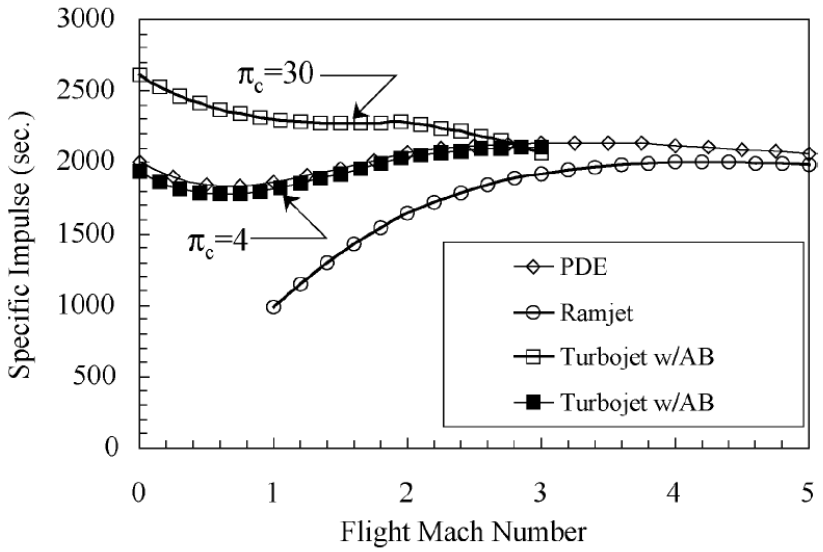

Figure 10. PDE, Ramjet and Turbojet Specific Impulse Performance as function of Mach Number (from Ref. [18])

And thus, the next chapters cover the experimental apparatus designed and built to carry out the thesis' motivation. The DDT performance of TPI is compared to that of a Capacitive Discharge spark plug (CD Spark) ignition system for reference. An additional concept that utilizes two TPI electrodes for ignition is discussed and evaluated.

THIS PAGE INTENTIONALLY LEFT BLANK

II. EXPERIMENTAL SETUP

This chapter covers the experimental set up utilized by the thesis. It describes the test facility, its systems and PDE combustor operation. Configurations tested are described and the thesis test matrix is discussed.

A. TEST CELL FACILITY

Testing for this thesis work was conducted at NPS' Rocket Propulsion Laboratory (RPL), test cell #1. The main experimental apparatus, a PDE combustor, was adapted in design to employ existing laboratory and test cell capabilities in control, air and fuel delivery, and data acquisition. Several internal combustor configurations were tested employing both a traditional CD Spark plug ignition system and a TPI system for ignition delay, mass flow ignition limits mapping, and stoichiometric ratio and DDT performance comparisons. All test firing runs were single-shots, a single cycle in the PDE operational cycle. Figure 10 shows an overall schematic of the experimental setup.

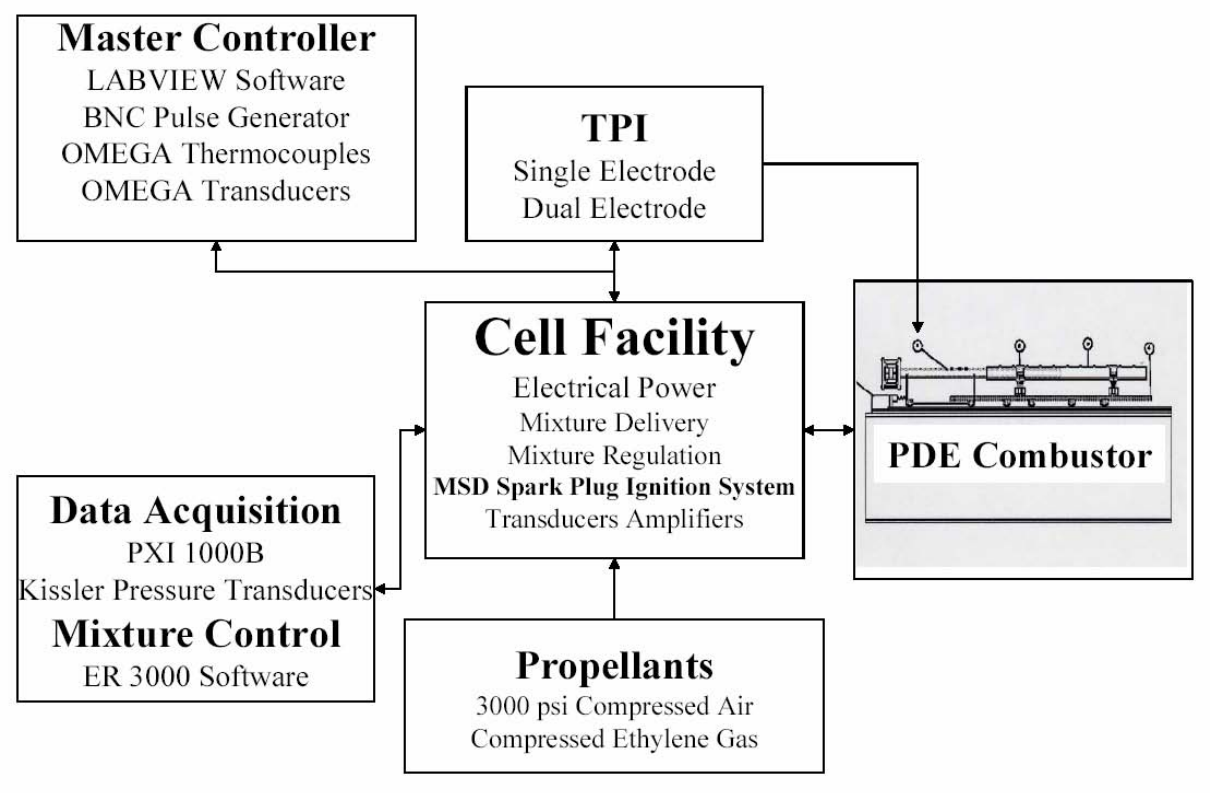

Figure 11. Experimental Setup Schematic

Test cell #1 delivered compressed ethylene gas, at slightly lean and rich concentrations, the chosen fuel for this thesis investigation. Ethylene is a readily available, easy to handle and well-characterized fuel that has an extensive research database. Harder to detonate than hydrogen/air, results from ethylene/air mixtures correlate suitably with that of desired liquid fuels for military PDE propulsion applications such as JP-5, JP-10, and Jet A. Additional ethylene technical data is provided in Appendix A.

1. Vitiator and Mixture Delivery

The test cell facility features a hydrogen/air vitiator capable of heating air flow to a maximum temperature of 1,000 ºF in order to simulate inlet temperatures a PDE would encounter during supersonic flight. High pressure inlet air is fed into the vitiator from four high-pressure (3000 psi) tanks through 2 inch stainless steel pipe. The vitiator system is comprised of a 2 inch stainless steel pipe section with welded steel flanges as shown in Figure 12. A stainless steel insert is fitted to the inside of the vitiator pipe which acts as a combustor can. The high pressure air mass flow is divided by a series of half inch diameter holes which divert 11% of the flow through the center of the insert and 89% of the remaining flow over the outside of the insert as shown in Figure 13. Hydrogen is injected into the insert through a port as annotated in Figure 12. A spark plug ignited hydrogen/air torch is used to ignite and burn the hydrogen/air mixture within the vitiator insert. The air flow on the outside of the insert is heated by convection. As air is used as the oxidizer in the vitiator, “make-up oxygen” is fed into the high pressure air pipe downstream of the vitiator to return the gaseous oxygen content in the air back to the approximately 21 % for engine or combustor operation [16]. This facility feature was not employed in this thesis’ test matrix but will be part of future TPI research work.

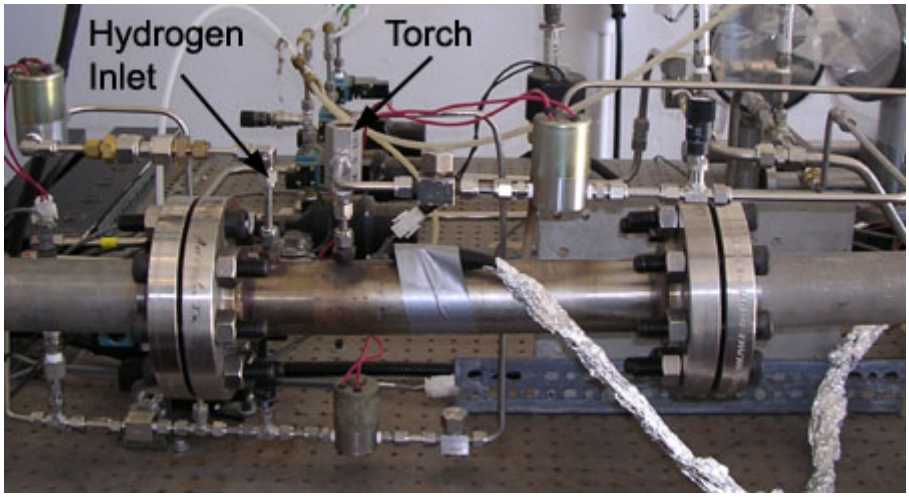

Figure 12. Vitiator Air Heating System (side view)

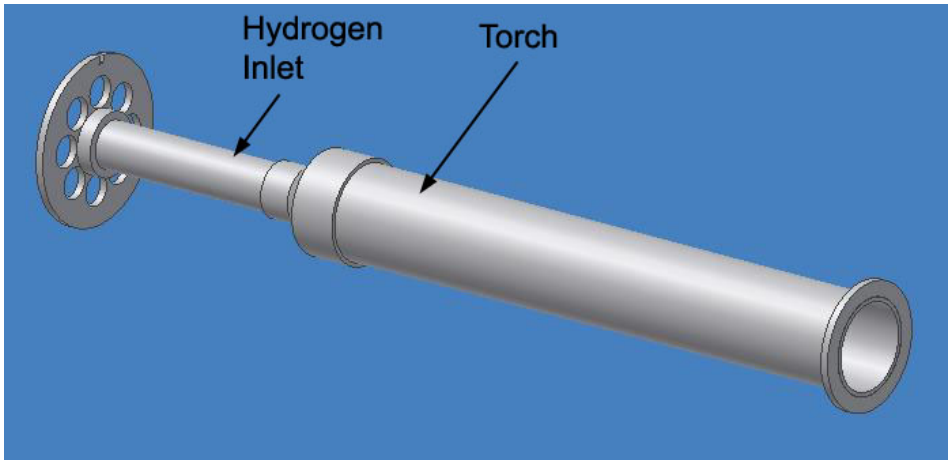

Figure 13. Vitiator Insert

After exiting the vitiator, the air mass flow is split into two flow paths and is reduced to 1.5 inch diameter piping. The air mass flow path then enters one of three manifolds. Splitting again into two 1 inch diameter lines, solenoid-valved fuel is injected from two fuel lines into the air mass flow where the two additional manifolds aid fuel/air mixture, each connecting to two 0.5 inch diameter combustor fuel/air mixture feed lines. Four check-valves protect the fuel/air mixture feed lines from potential combustor blow back upstream.

This setup is shown in closer detail in Figure 13. Air flows from the 2 inch diameter piping (shown in upper left) into the combustor (shown in lower right). The flow path of the air delivery system is split into two flow paths in order to eliminate the

effect of the compressed and vitiated air flow on test stand thrust measurements when taken. Thrust measurements were not made in this thesis.

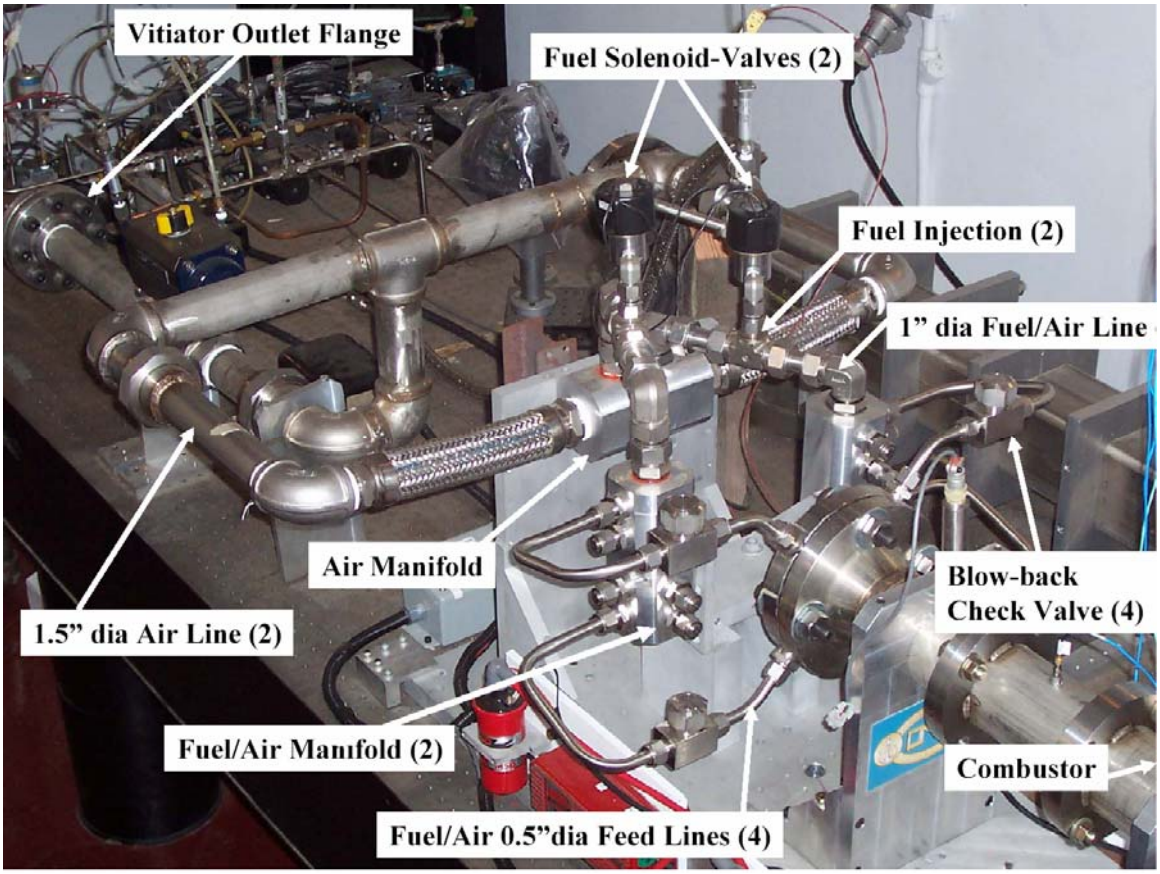

Figure 14. PDE Combustor Air Delivery Setup (top view)

2. Mass Flow Regulation and Equivalence Ratio

A 0.236 inch diameter mass flow metering choke was placed in the main high pressure air line upstream of the vitiator for air mass flow control. Likewise, 0.052 inch diameter chokes meter ethylene flow in the combustor two fuel lines. Mass flow for compressible fluids, assuming isentropic flow, was calculated with the following equations in simplified form [16].

$$\dot{m} = \left(\frac{A_2 p_t}{T_t^{1/2}} \right) \Gamma_2 K_\Gamma \tag{4}$$

$$K_\Gamma = \left[\left(\frac{g_c}{R} \right) \left(\frac{2\gamma}{\gamma - 1} \right) \left(\frac{2}{\gamma + 1} \right)^{2/(\gamma - 1)} \left(\frac{\gamma - 1}{\gamma + 1} \right) \right]^{1/2} \quad (5)$$

where:

$\dot{m}$ = mass flow

γ = Ratio of specific heats

R = Specific gas constant

g_c = Gravity acceleration constant

A_2 = choke area

T_t = Total temperature

p_t = Total pressure

The mass flow calculations assumed that total temperature and pressure were those at the upstream conditions with Γ_2 was set equal to one. To account for losses, facility calibration runs were completed to compare actual mixture flows profiles with theoretical calculated flows.

Fuel richness or concentration is known as the equivalence ratio. Equivalence ratio, ϕ, is defined as the molar ratio of fuel to oxidizer in the used mixture, divided by the molar ratio of fuel to oxidizer in a stoichiometric mixture as shown below in Equation (6).

$$\phi = \frac{\dfrac{fuel}{oxidizer}}{\left[\dfrac{fuel}{oxidizer}\right]_{stoichiometric}} \quad (6)$$

A stoichiometric mixture is one where all of the chemical reactants are used to completion to complete the combustion process. An ethylene (C_2H_4) air ($O_2 + 3.76N_2$) mixture was used for combustion during testing. The stoichiometric relationship shown below with the equation balanced appropriately as:

$$C_2H_4 + 3(O_2 + 3.76N_2) \rightarrow 2CO_2 + 2H_2O + 3 \cdot 3.76N_2 \quad (7)$$

In this case, the stoichiometric ratio is found by calculating the fuel to air mass ratio of the reactants.

$$\left[\frac{fuel}{oxidizer}\right]_{stoichiometric} = \frac{(24+4)}{3(32+3.76\cdot 28)} = 6.79\% \quad (8)$$

To set a specific mixture equivalence ratio for testing, accurate mass flow of fuel and air must be determined using the calculation methods described above and set manually by the setting of appropriate upstream metering chokes pressures using the flow regulation control system (ER3000).

Actual fuel and air, and thus total mass flow quantities for a given test run may be determined by recalculating the parameters using actual pressures and combustor conditions data logged during the run. With both actual fuel and air mass flow rates, the actual fuel to oxidizer ratio was found by dividing the two, and thus determining the actual equivalence ratio by dividing the actual fuel to oxidizer ratio by the stoichiometric value of 6.79 percent.

3. Facility Control and Data Acquisition

A robust, high-speed network was required to safely control, operate and evaluate the PDE combustor. National Instruments LABVIEW 7.1 software was used for facility control and data logging. ER 3000 software and component suite was used for mixture flow regulation. Both of these software programs were operated at computer terminals in the Laboratory's control room with additional manual safety, "man in the loop", shutoff switched and power source breakers.

The LABVIEW software is networked to a National Instruments PXI 1000B with a NI PXI-8176 Embedded Controller. The PXI controls a NI PXI 6031E Multi-function I/O Data Acquisition card, a NI 6508 I/O signal output card, and a NI 6115 Simultaneous Sampling Multifunction I/O high speed data acquisition card. The NI PXI 1000B is shown in Figure 15. The NI 6508 I/O card provides 5 volt output signals controlled by the LABVIEW code to manually or automatically open and close AC and DC solenoid and ball valves. The NI 6508 I/O signal output card is shown on the left in Figure 16.

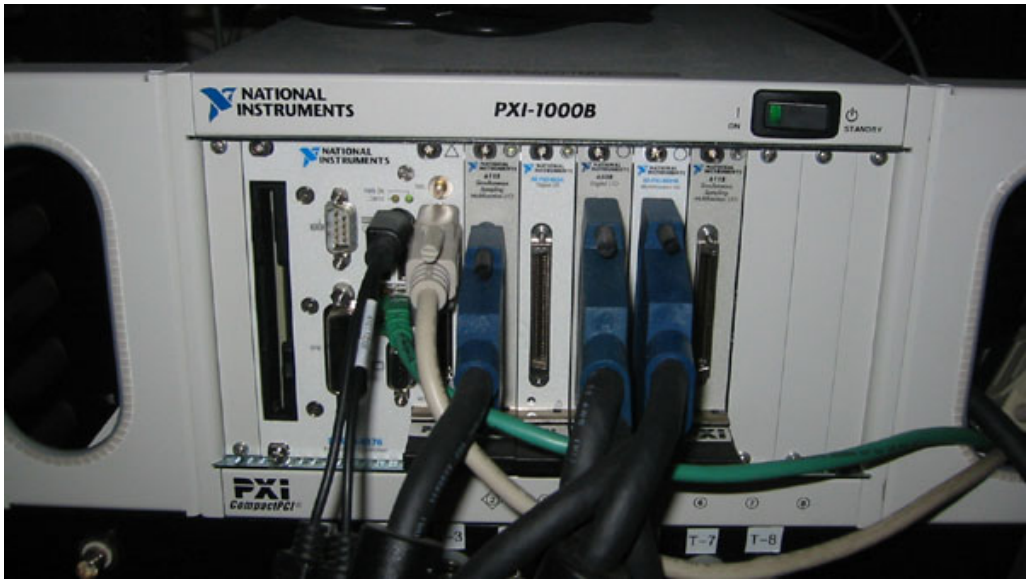

Figure 15. National Instruments PXI 1000B

The NI PXI 6031E Multifunction I/O Data Acquisition card samples multiple channels of voltage data acquisition which are sent through a conversion factor in LABVIEW software for pressure and temperature high-speed data logging. OMEGA PX613 pressure transducers and OMEGA HGKMQSS Type K thermocouples were used to acquire data with this card. The NI 6031E data acquisition card is shown on the right in Figure 16. Kissler amplifiers at the facility and pressure transducers at the PDE combustor were used for high speed pressure readings at frequencies of up to 10 megahertz (MHz).

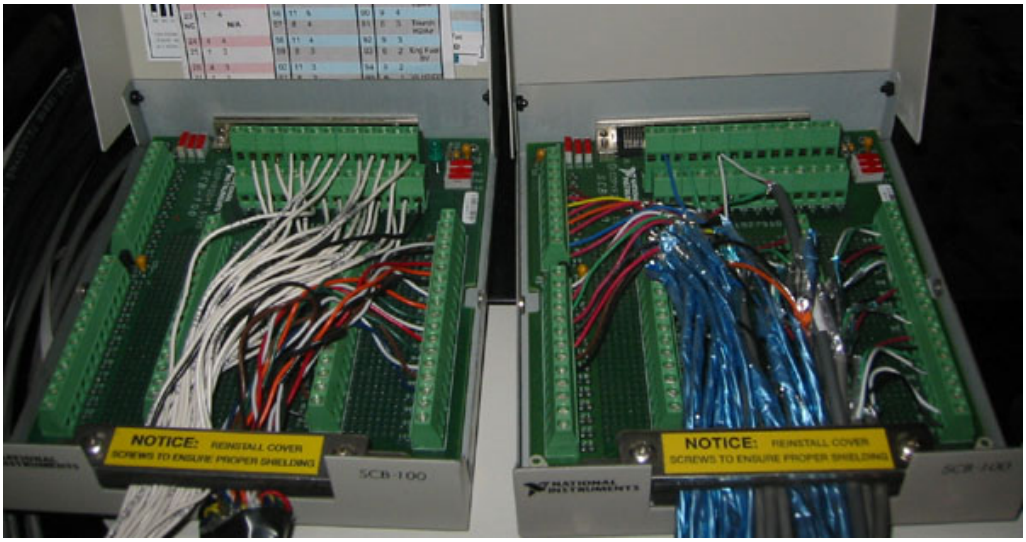

Figure 16. National Instruments 6508 I/O Signal Output and 6031E Multifunction I/O Data Acquisition Cards

Precise control of two solenoid valves to inject ethylene fuel, data logging start, and ignition triggering of both the MSD CD Spark and TPI systems was vital for correct timing in each single-cycle test firing. The proper timing was accomplished by the network's BNC Model 500 Pulse Generator, controlled by the LABVIEW software. Figure 16 shows the BNC Model 500 Pulse Generator.

Figure 17. BNC Model 500 Pulse Generator

Figure 17 shows the LABVIEW master controller terminal graphical user interface. This manual version allows manual opening and closing of all supply gas and main air ball valves. The vitiator is controlled in an automated stacked sequence which allows for inputs of vitiator and torch operation time. Enabling of the test cell power is also controlled with the virtual instrument through a manual switch which also simultaneously opens the engine main air ball valve to provide a step of safety. Supply gas, torch igniter, and choke pressures are displayed and logged at 100 Hz. Choke and engine temperatures are also displayed and logged at 100 Hz. More detail of the LABVIEW code is shown in Appendix B.

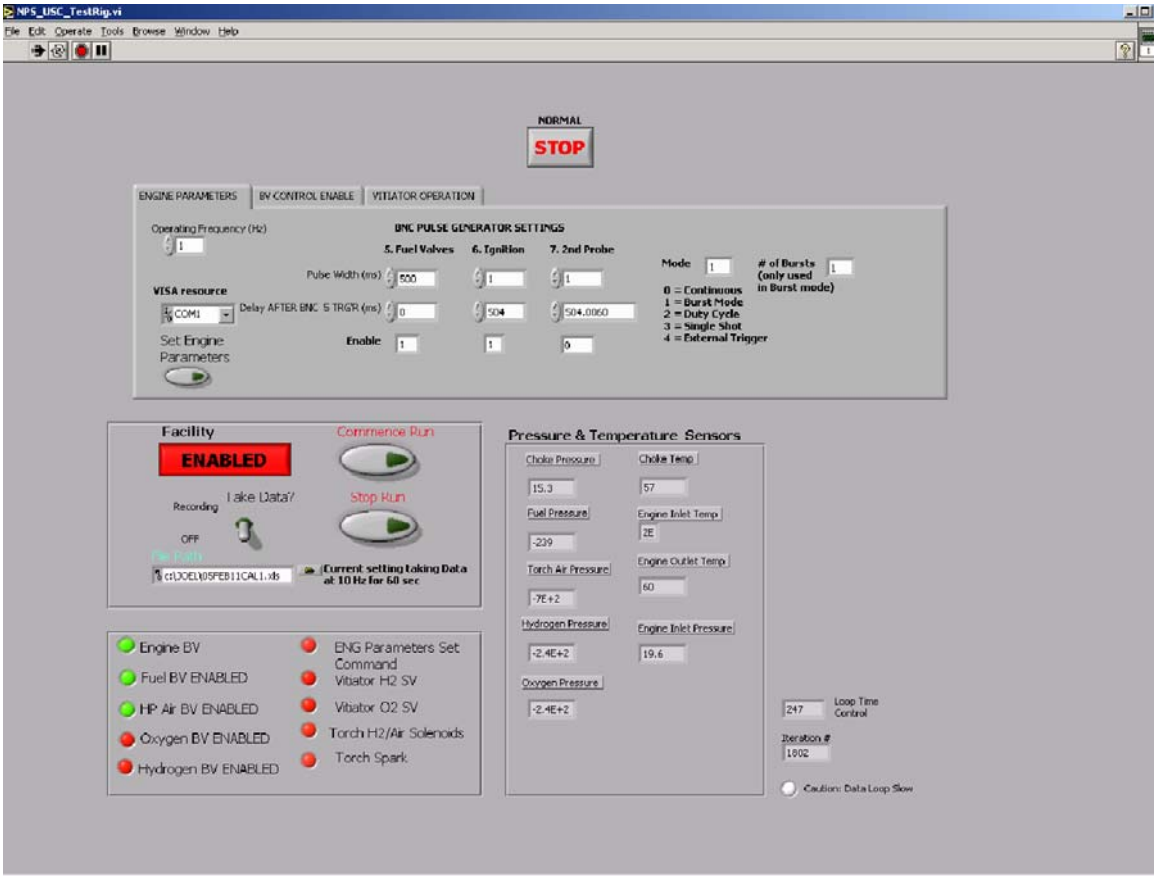

Figure 18. LABVIEW Software Control Window Panel

B. DESIGN OF MODULAR PDE COMBUSTOR

The PDE combustor was made of 7 flanged 3-inch diameter Schedule 40 stainless steel tube segments. This diameter was chosen in order to support cell size detonation structures for a variety fuels besides ethylene. Follow-on research, for instance, may

employ a propane/air mixture which is a more surrogate mixture for the desired aviation turbine (grade JP) fuels for PDEs.

Several segments configurations were possible and employed. The design called for an 8 inch long head-end segment and 6 other segments: two segments each of 3, 6 and 9 inches in length. Each of the segments is able to accommodate a DDT obstacle device insert. Utilizing the modularity of the design, the internal DDT obstacle length can be easily and practically varied from no length to 3, 6, and 9 and so forth up to 36 inches in increments of 3 inches of length by combustor configuration changes.

The DDT obstacle inserts are shown in Figure 18. They are segmented Chin spirals supported by a single 0.125 thick washer and outside welds to four 0.25 inch diameter stainless steel rods, each 45 degrees apart. The spirals are made of 0.125 inch diameter treated stainless steel wire, an inner diameter of 2.40 inches and an outer diameter of 2.65 inches. With a pitch of 2.95 inches, the spiral coil spacing is roughly one tube diameter as proven near-optimal for DDT obstacle spacing by past PDE research. The custom-made spirals were acquisitioned from Newcomb Spring of California.

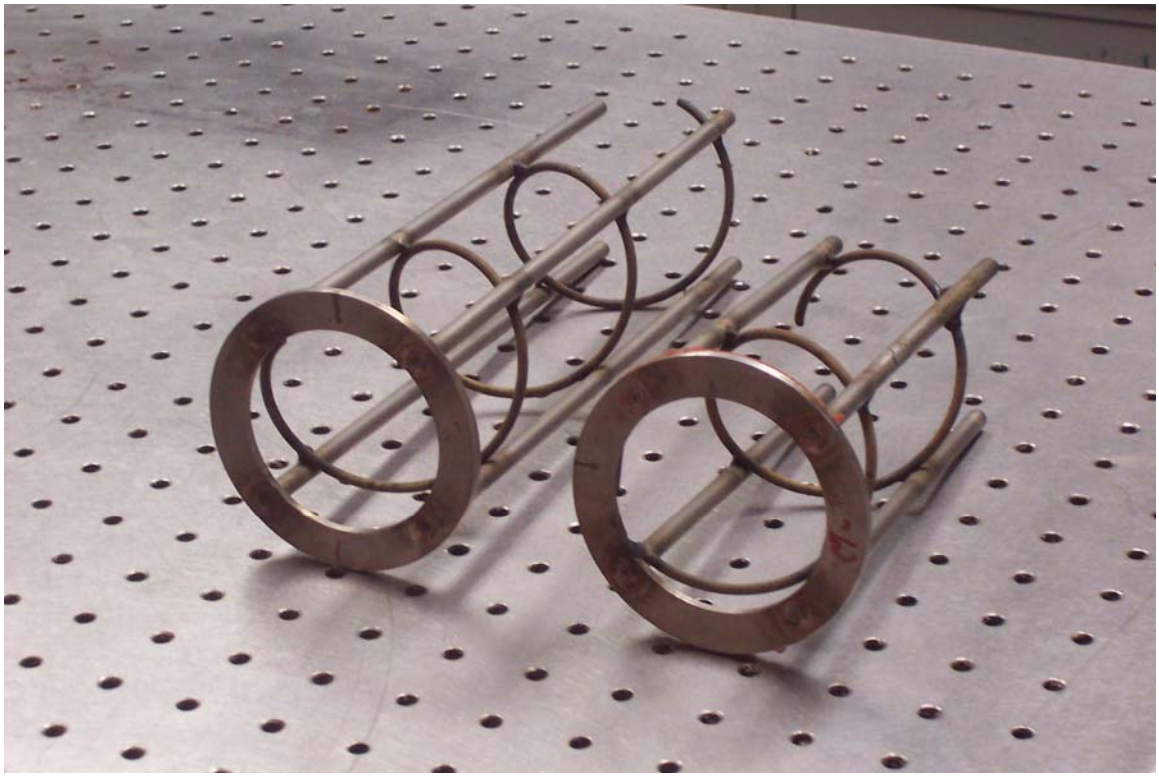

Figure 19. Nine and six inches long PDE Combustor Chin Spiral DDT Obstacle Inserts

C. TEST CONFIGURATIONS

1. CD Spark Plug Configuration

One PDE combustor configuration was tested using the electrical capacitance discharge spark plug ignition system. The configuration was made up of seven segments. Overall combustor length was 1.13 meters with a 0.914 meters long DDT internal obstacle. Ethylene, air, engine inlet and outlet temperatures. Seven high- speed data Kissler pressure transducers recorded combustor pressures. The CD Spark Plug Configuration is shown in Figure 19.

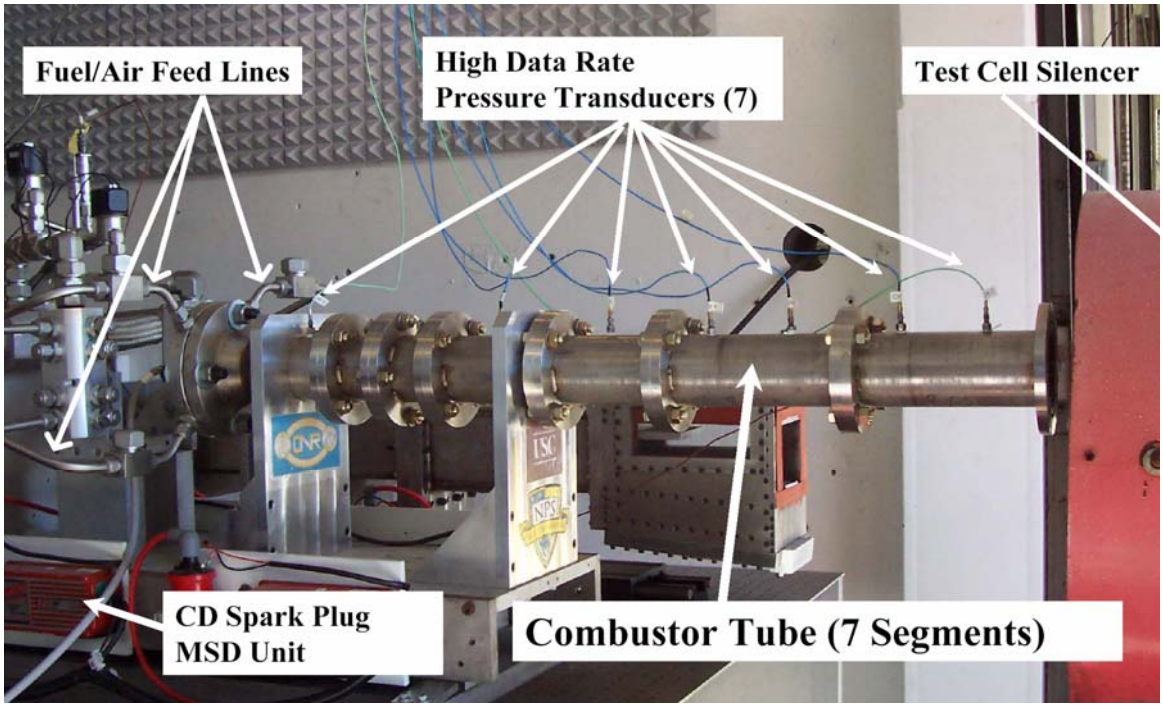

Figure 20. CD Spark Plug Configuration

One Champion RN12YC spark plug was installed in the combustor's head flange center. The spark plug was ignited by a high-performance automobile MSD ignition system. The MSD 6 Series feature a capacitive discharge ignition design. Most ignition systems available in the market are inductive systems which result in spark misses at high frequency operation. When required in the future, the MSD system used in this configuration will be capable to support multi-cycle operation.

2. TPI System

The TPI pulse generator is designed to deliver pulses of 70 kV in amplitude for 50 nanoseconds. In order to avoid occasional arcs, the output impedance of the generator is

matched to the load, so peak currents are limited to twice the operating current. The pulse shape is relatively unimportant. The rise time, repetition rate, and reliability requirements can be met using pseudo-spark switch. The final pulse amplitude is achieved by using a pulse transformer [19]. Figure 20 shows a typical TPI pulse profile.

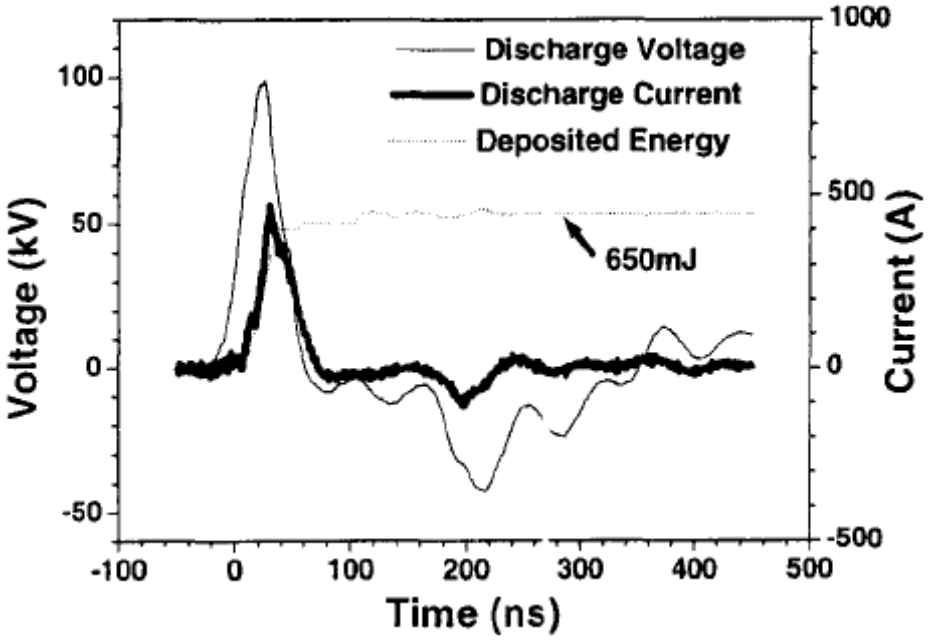

Figure 21. Typical 50 nanosecond TPI Pulse Profile (from Ref.[19])

a. Single Electrode TPI Configuration

One single TPI configuration was tested. The PDE combustor configuration was identical to the one described above with the CD Spark ignition system. The only obvious exception is that of the ignition system. The spark plug was replaced by a 76 mm long, 4 mm diameter stainless steel TPI electrode.

b. Dual Electrode TPI Concept and Configurations

The concept of using a second electrode to aid in ignition was implemented in a set of configuration. A second electrode was placed before a detonation wave was sure not to have developed. The rational for this concept was the determination of whether a second TPI ignition source, triggered at an appropriate time delay from the first electrode, would result in the acceleration of the DDT process. Due to the electrical

insulation required by this second electrode, its implementation added an obstacle with approximately 40% combustor flow path blockage.

Seven configurations utilizing the dual electrode TPI concept were tested. In six of the configurations, the first electrode spanned from x/D = 0 to 0.98, L1,(where x is horizontal location on PDE combustor, D is combustor inner diameter of 3.063 inches) and the second electrode from x/D = 3.48 to 3.81 (L2) at centerline with various internal DDT obstacles configurations. One configuration tested the TPI concept with the first electrode spanning from L1 and the second electrode from x/D = 6.42 to 6.75 (L3).

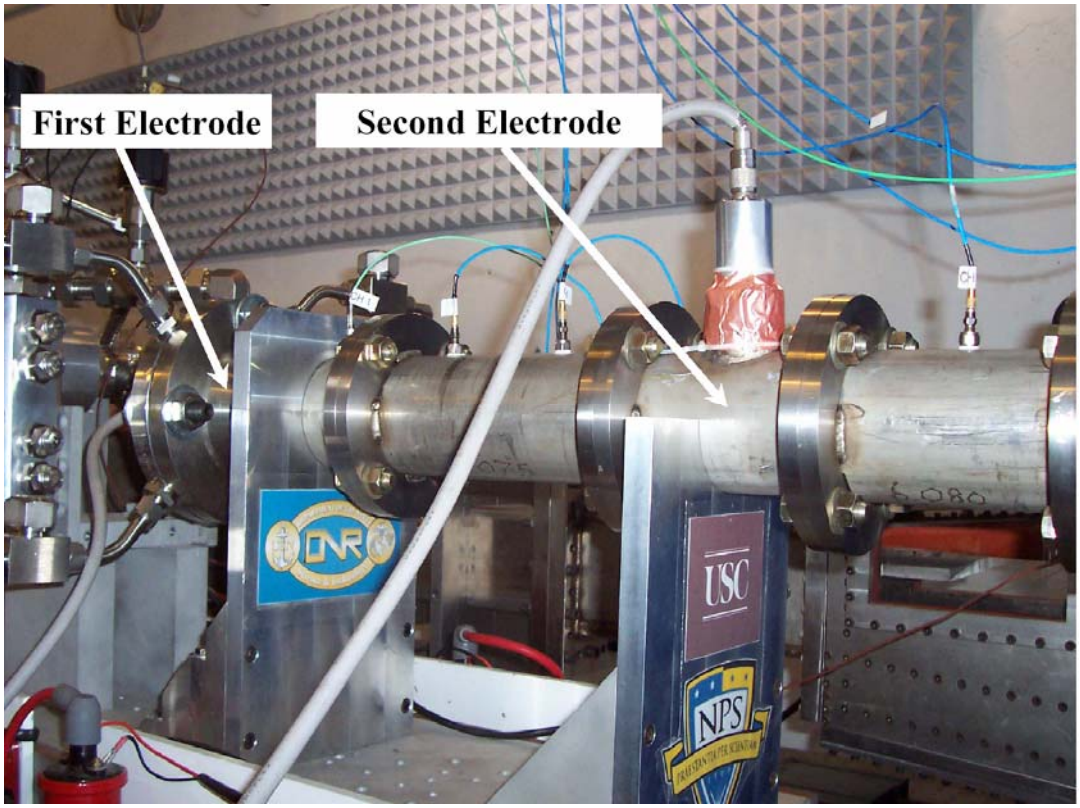

Figure 22. Dual TPI Electrode Configuration (L1 and L3 configuration)

D. TEST MATRIX

For the CD Spark ignition system, three independent variables were investigated: mass flow, mixture equivalence ration and the length of internal obstacles required for successful DDT. Table 1 lists the specific conditions tested for each parameter.

A similar test matrix, shown in Table 2, was applied for TPI. Two additional variables were investigated: second electrode ignition trigger delay and second electrode location.

Variable	**Values Investigated**	**Units**
Mass flow	0.025, 0.050, 0.075, 0.1,0.2, 0.3, 0.4 and 0.5	kg/s
Equivalence Ratio	0.8, 0.95, 1.0, 1.025, 1.05, 1.10 and 1.2	N/A
Internal DDT Obstacle Length	Minimum for DDT	Inches
Ignition Delay	N/A	milliseconds

Table 1. CD Spark System Test Matrix

Variable	**Values Investigated**	**Units**
Mass flow	0.025, 0.050, 0.075, 0.1,0.2, 0.3, 0.4 and 0.5	kg/s
Equivalence Ratio	0.8, 0.95, 1.0, 1.025, 1.05, 1.10 and 1.2	N/A
Internal DDT Obstacle Length	Minimum for DDT	inches
Ignition Delay	N/A	milliseconds
Second Electrode Ignition Trigger Delay	0.35, 0.45, 0.50, 0.55, 0.65, 0.70 and 0.75	milliseconds
Second Electrode Location	L2 or L3	x/D

Table 2. TPI Test Matrix

III. RESULTS & DISCUSSION

A. RESULTS

Figure 22 shows typical combustor pressure traces and provides a sample of the high-speed data acquisition system product. Using such traces, it was determined whether detonation did occur, detonation wave velocity, ignition delay time, and DDT distance and time were estimated.

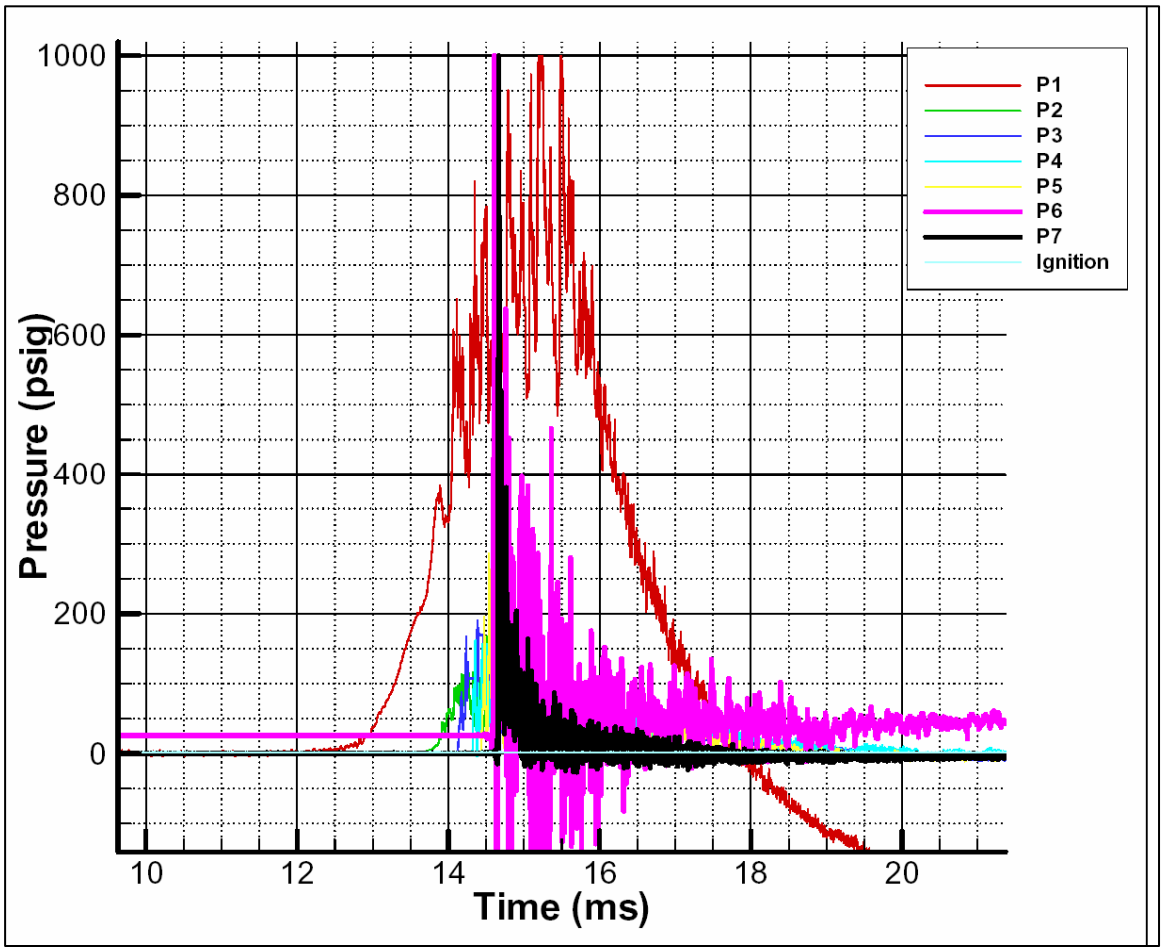

Figure 23. CD Spark Ignition System Test Run 6

Detonation velocity, V_{det}, was determined using Equation (9), where Δx is the known distance between two transducers which traces indicate a fully developed detonation wave; and Δt is the time delay between them as measured from the trace plot. The P1 transducer was set at higher sensitivity (10 units per Volt) in order to

determine ignition delay, defined in this thesis as an initial pressure rise of 4 atmospheres (50 psig). Further analysis of pressure traces' magnitude and location yielded DDT location and DDT time estimates. Due to the volume of the data, up to 1.75 million points per run, data analysis required extensive resolution manipulation of data acquisition and plotting software.

$$V_{det} = \frac{\Delta x}{\Delta t} \tag{9}$$

B. DISCUSSION

Figure 23 compare CD Spark, Single TPI and Dual TPI DDT performance as a function of mass flow. CD Spark data supports previous NPS research data with limited success at mass flow rates higher than 0.137 kg per second. CD Spark ignition had an overall detonation success rate of 37% as opposed to 94% detonation success rate on TPI configurations. The TPI configurations allowed for tests at maximum flow rates of the current facility.

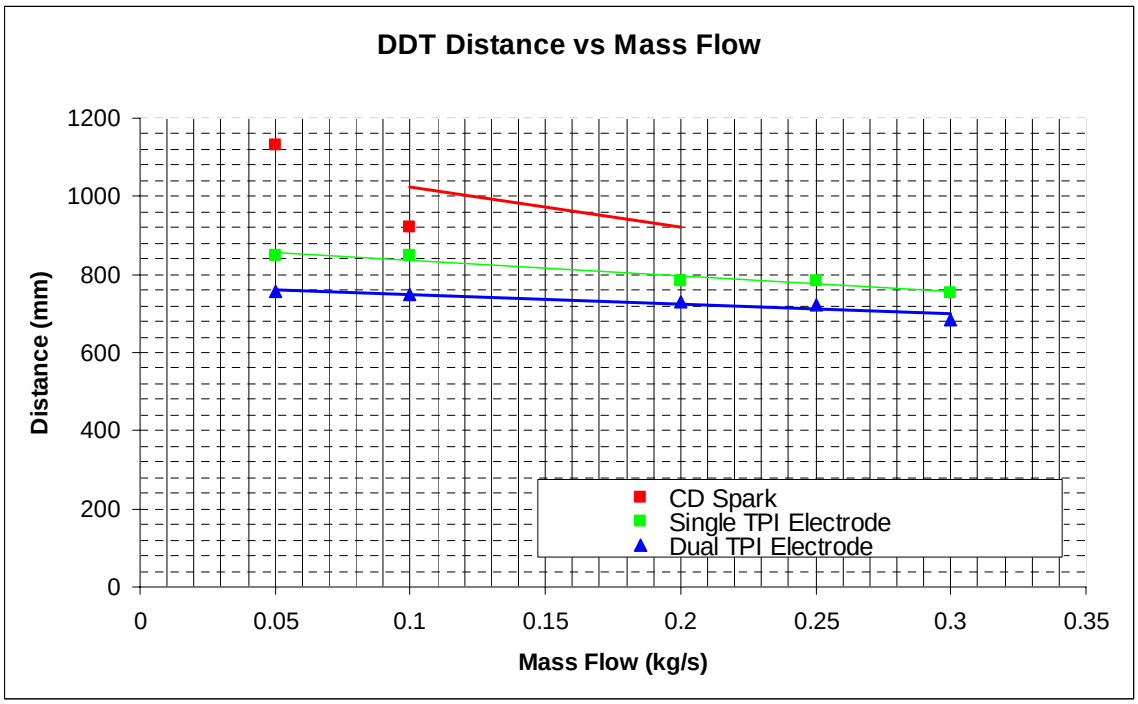

Figure 24. DDT Distance Performance vs. Mass Flow for CD Spark, Single TPI and Dual TPI Configurations

In the Dual TPI configuration, an optimum time delay range between electrode discharges determined. For theL1-L2 configuration, the optimum time delay range is from 555 to 610 microseconds. Performance of the L1-L3 configuration did not surpass the previous configuration and was comparable to single TPI electrode performance.

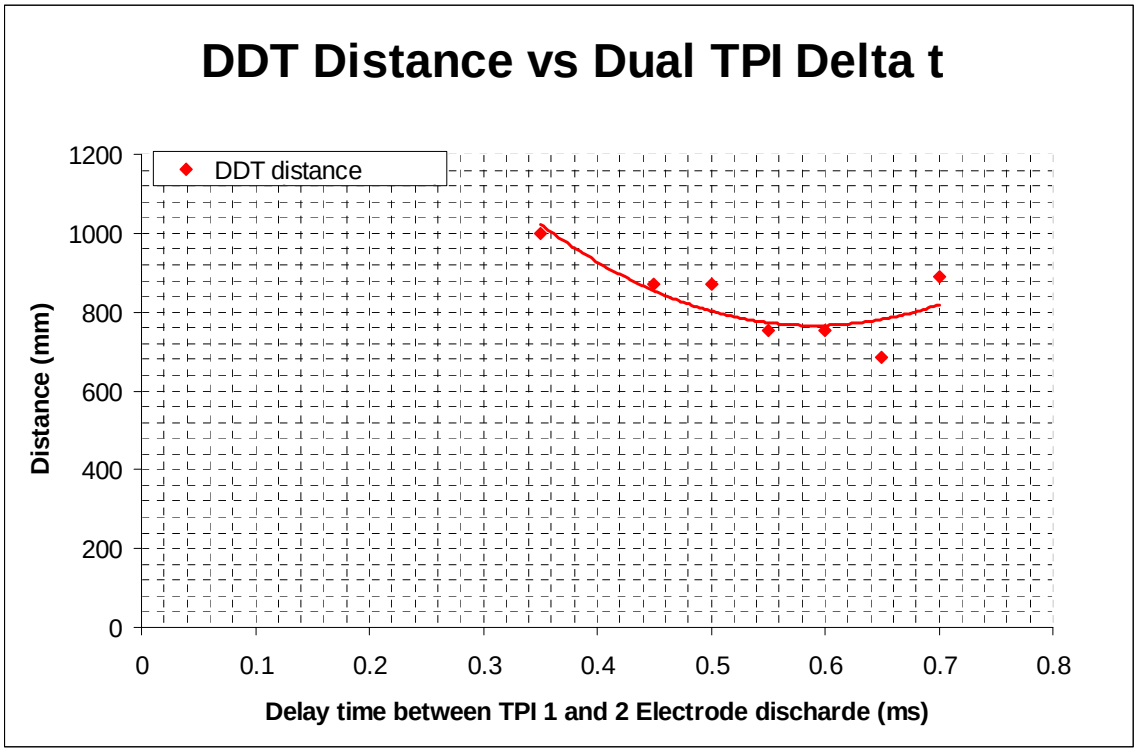

Figure 25. Determination of Optimum Discharge Time Delay between Electrodes for Dual TPI Configuration

A difference in ignition delay was observed in between the Single and the Dual TPI configurations as a function of equivalence ratio, Figure 25. This is due to the combination of the following factors: the change of downstream conditions due to the second ignition source and a different combustor back-pressure due to the second electrode's dielectric feed-through fitting, an obstacle in the PDE's combustor flow.

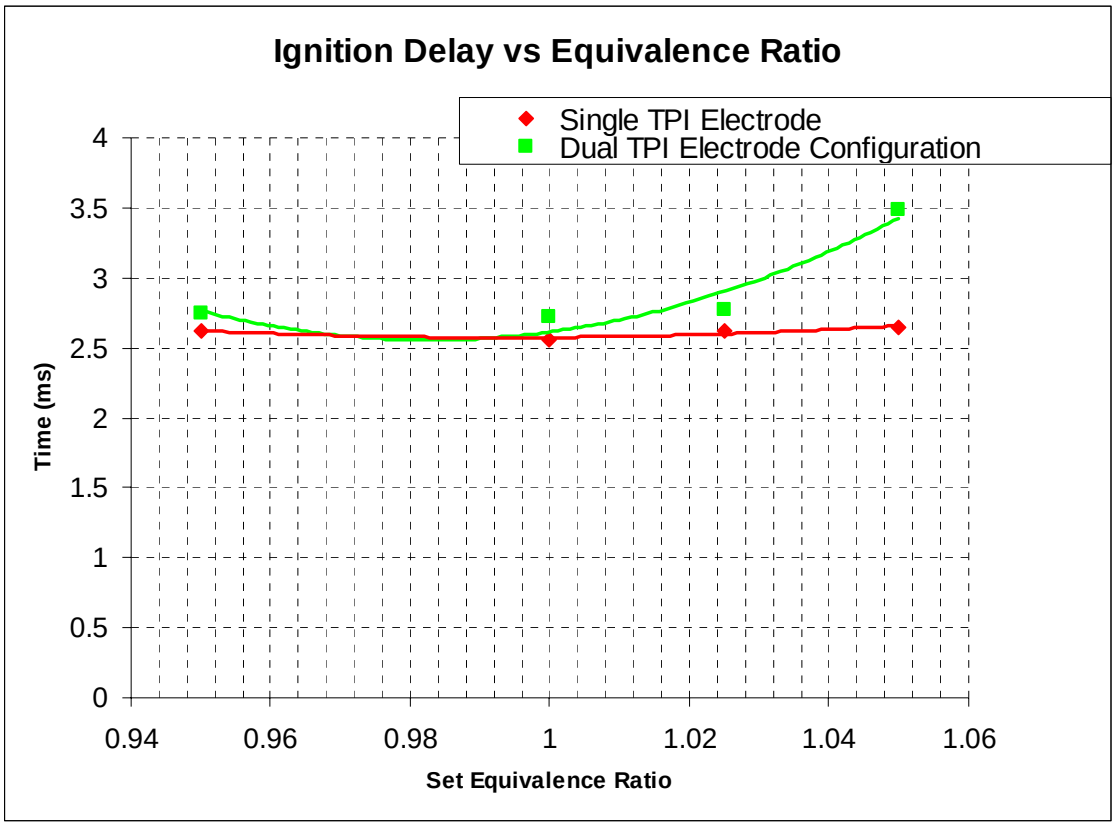

Figure 26. Ignition Delay as a function of Equivalence Ratio for Single and Dual TPI Configurations

Combustor back-pressure did prove to be a critical factor in several test runs where no DDT obstacles were present and both Single and Dual TPI failed to ignite the mixture. When a single obstacle, a simple insert washer, was inserted the mixture did ignite and failed to detonate.

IV. CONCLUSIONS

Transient Plasma Ignition technology has been proven to be more effective and reliable than a high-performance Capacitive Discharge spark plug ignition system. A noteworthy improvement in DDT performance proves that TPI, if scalable, will remove most if not all of the auxiliary oxygen requirements. Single TPI configurations when compared to CD Spark runs, reduce DDT distance by an average of almost 10% (~100 mm) and DDT time by and average 33% (~5 milliseconds).

When the electrodes were set at L1 and L2, the dual TPI configuration did successfully accelerate the DDT process. When compared to CD Spark runs, DDT distance and time was reduced by 17 % (~170 mm) and 41% or ~6.15 milliseconds respectively. The feasibility of this configuration was proven; some of its complexities in terms of physical interface and precise timing requirements were also encountered.

TPI does appear to be significantly sensitive to combustor back-pressure but due to diagnostic limitations, this issue could not be investigated further in this thesis.

THIS PAGE INTENTIONALLY LEFT BLANK

V. FUTURE WORK

The next steps to further this thesis effort would entail further testing of the present configurations at different temperature conditions (vitiated air) using ethylene/air, and propane/air. Additional combustor instrumentation designed to monitor combustor back-pressure conditions will be best. Eventually, after assessing and taking into account the material and operational lessons learned from this PDE combustor, a geometry that corresponds to the NPS Valveless PDE design initiator should be pursued by itself with the physical and material flexibility for full-scale implementation with the engine.

THIS PAGE INTENTIONALLY LEFT BLANK

LIST OF REFERENCES

[1] Kailasanath, K., "Recent Developments in the Research on Pulse Detonation Engines," *AIAA Journal*, v. 41, pp. 145-159, February 2003.

[2] Hoffmann, H., "Reaction-Propulsion Produced by Intermittent Detonative Combustion," German Research Institute for Gliding, ATI-52365, August 1940.

[3] Nicholls, J.A., Wilkinson, H.R., and Morrison, R.B., "Intermittent Detonation as a Thrust-Producing Mechanism," *Jet Propulsion*, pp. 534-541, May 1957.

[4] U.S. Naval Ordnance Test Station NAVWEPS Report 7655, AD-284312, *Performance Characteristics on an Intermittent-Detonation Device*, by L.J. Krzycki, June 1962.

[5] Helman, D., Shreeve, R.P., and Eidelman, S., "Detonation Pulse Engine," AIAA paper 1986-1683, June 1986.

[6] Cambier, J.L., and Adelman, H.G., "Preliminary Numerical Simulations of a Pulsed Detonation Wave Engine," AIAA paper 1988-2960, July 1988.

[7] Bussing, T., and Pappas, G., "An Introduction to Pulse Detonation Engines," AIAA Paper 1994-0263, 32nd AIAA Aerospace Sciences Meeting and Exhibit, Reno, Nevada, 10-13 January 1994.

[8] Roy, G.D., "Status of Navy PDE Research," PowerPoint presentation at Office of Naval Research PDE Workshop, Dayton, Ohio, 12 September 2002.

[9] "Ash Cleaning: Pratt & Whitney Ash and Slag Detonation Online Cleaning System." [http://www.pratt-whitney.com/serv_sms_ash.asp]. 28 February 2005.

[10] van Wingerden, K., Bjerketvedt, D., and Bakke, J.R., "Detonations in Pipes and in the Open," Christian Michelsen Research paper, Bergen, Norway.

[11] Kuo, K.K., *Principles of Combustion*, pp. 231-273, John Wiley & Sons, Inc., 1986.

[12] Fickett, W., and Davis, W.C., *Detonation*, pp. 13-16, University of California Press, 1979.

[13] Brophy, C.M., Werner, S., and Sinibaldi, J.O., "Performance Characterization of a Valveless Pulse Detonation Engine," AIAA paper 2003-1344, 41st AIAA Aerospace Sciences Meeting and Exhibit, Reno, Nevada, 6-9 January 2003.

[14] Higgins, A.J., Pinard, P., Yoshinaka, A.C., and Lee, J.H.S., "Sensitization of Fuel-Air Mixtures for Deflagration-to-Detonation Transition," in G. Roy, S. Frolov, D. Netzer, and A. Borisov (Eds.), *High-Speed Deflagration and Detonation: Fundamentals and Control*, pp. 45-49, ELEX-KM Publishers, 2001.

[15] Brophy, C.M., Sinibaldi, J.O., Ma, L., and Klingbeil, A.E., "Effects of Non-Uniform Mixture Distributions on Pulse Detonation Engine Performance," AIAA paper 2005-1304, 43rd AIAA Aerospace Sciences Meeting and Exhibit, Reno, Nevada, 10-13 January 2005.

[16] De La Rosa, J.G., *Development of a Shock Focusing Geometry Using Supersonic Jet Initiation for a Pulse Detonation Engine*, Master's Thesis, U.S. Naval Postgraduate School, Monterey, California, December 2004.

[17] Brophy, C., Sinibaldi, J.O., Wang, F., Jiang, C., and Gundersen, M.A., "Transient Plasma Ignition of a Hydrocarbon-Air Initiator for Pulse Detonation Engines," in G. Roy, S. Frolov, and J. Shepherd (Eds.), *Application of Detonation to Propulsion*, pp. 212-218, Torus Press, 2004.

[18] Paxson, D.E., "Performance Evaluation Method for Ideal Airbreathing Pulse Detonation Engines," *Journal of Propulsion and Power*, v. 20, pp. 945-947, September-October 2004.

[19] Wang, F., Kuthi, A., and Gundersen, M.A., "Technology for Transient Plasma Ignition," AIAA paper 2005-0951, 43rd AIAA Aerospace Sciences Meeting and Exhibit, Reno, Nevada, 10-13 January 2005.

[20] Starikovskaia, S.M., Kosarev, I.N., Krasnochub, A.V., Mintoussov, E.I., and Starikovskii, A.Y., "Control of Combustion and Ignition of Hydrocarbon-Containing Mixtures by Nanosecond Pulsed Discharges," AIAA paper 2005-1195, 43rd AIAA Aerospace Sciences Meeting and Exhibit, Reno, Nevada, 10-13 January 2005.

[21] "Detonation database**.** Technical Report FM97-8, GALCIT, July 1997" [http://www.galcit.caltech.edu/detn_db/html/]. 16 February 2005.

THIS PAGE INTENTIONALLY LEFT BLANK

APPENDIX A: ETHYLENE FUEL DATA

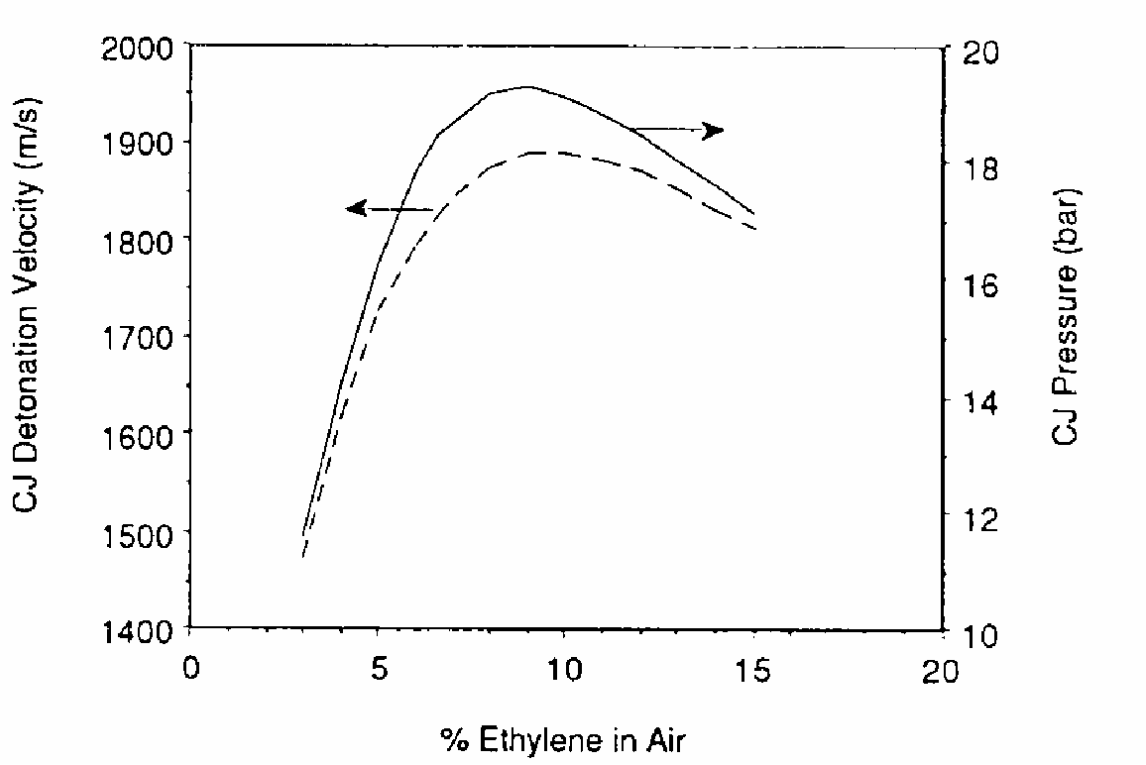

Figure 27. Ethylene/Air CJ Detonation Velocity and Pressure (from Ref. [10])

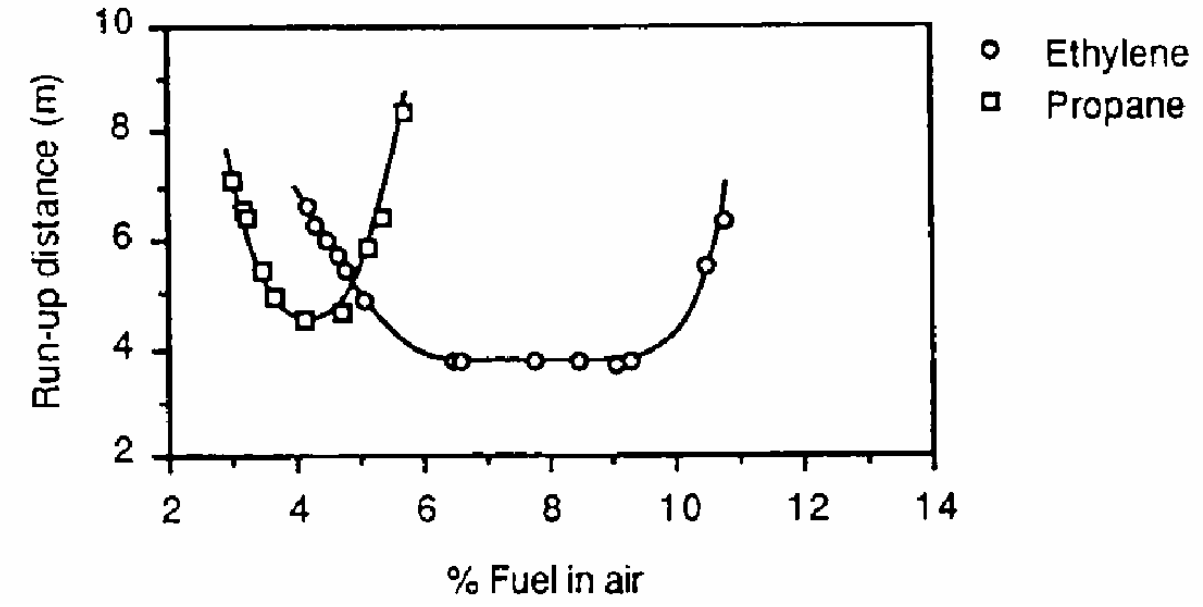

Figure 28. Smooth 1.96”-diameter Tube DDT Distance Ethylene/Air, Propane/Air Comparison (from Ref. [10])

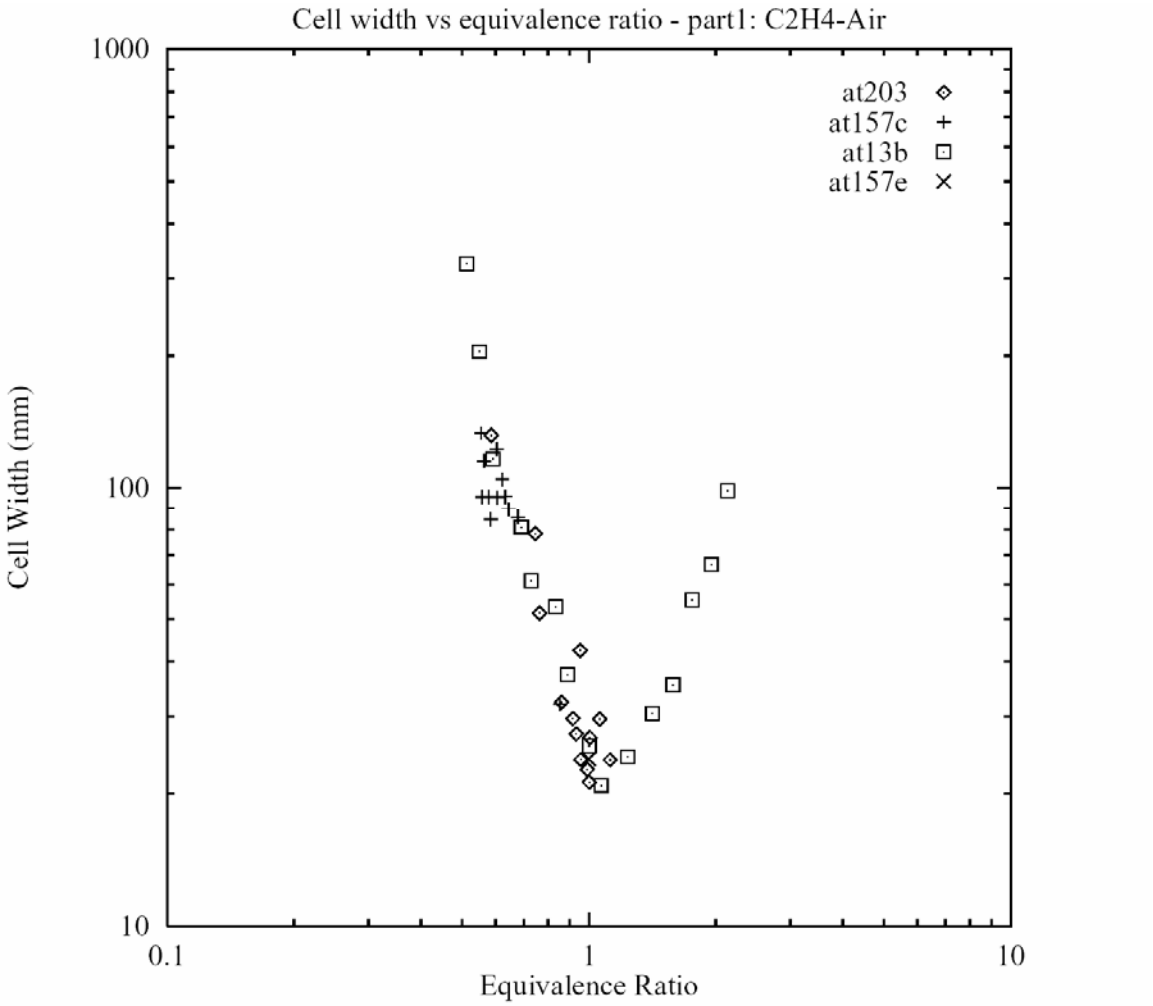

Figure 29. Several Observations of Ethylene/Air Cell Size vs. Equivalence Ratio (from Ref. [21])

APPENDIX B: LABVIEW CODE AND DESCRIPTION

LABVIEW version 7.1 was used for facility and engine control and diagnostics. Figure 30. shows the graphical user interface that was used to run the code. The three figures mentioned above all provide supply gas low speed pressure readings, temperature at the main air choke and in the engine, pressures in rocket igniters one, three, and four, and pressure in the reservoir. A main stop button stops the four main loops of the code. A facility enable/disable switch turns power on and off in the test cell and provides the same function as the manual "kill switch" on the wall of the control room of building 217. Commence and Stop run switches start and stop the BNC pulse generator which controls the fuel injection solenoid valves and MSD trigger. There is also a switch to start and stop data logging and an input block to specify the file name to write data to. There are also indicators to show when valves are opened or closed and status of the BNC pulse generator.[

The tabbed folder feature allows multiple screens of functions to be added to the graphical user interface (GUI). Figure 30. shows the tab which has inputs to set the parameters of the BNC pulse generator via LABVIEW shows the tab where all of the ball valves can be manually opened or closed. It is important to note that the main air ball valve was designed to open automatically when the facility was enabled for safety reasons

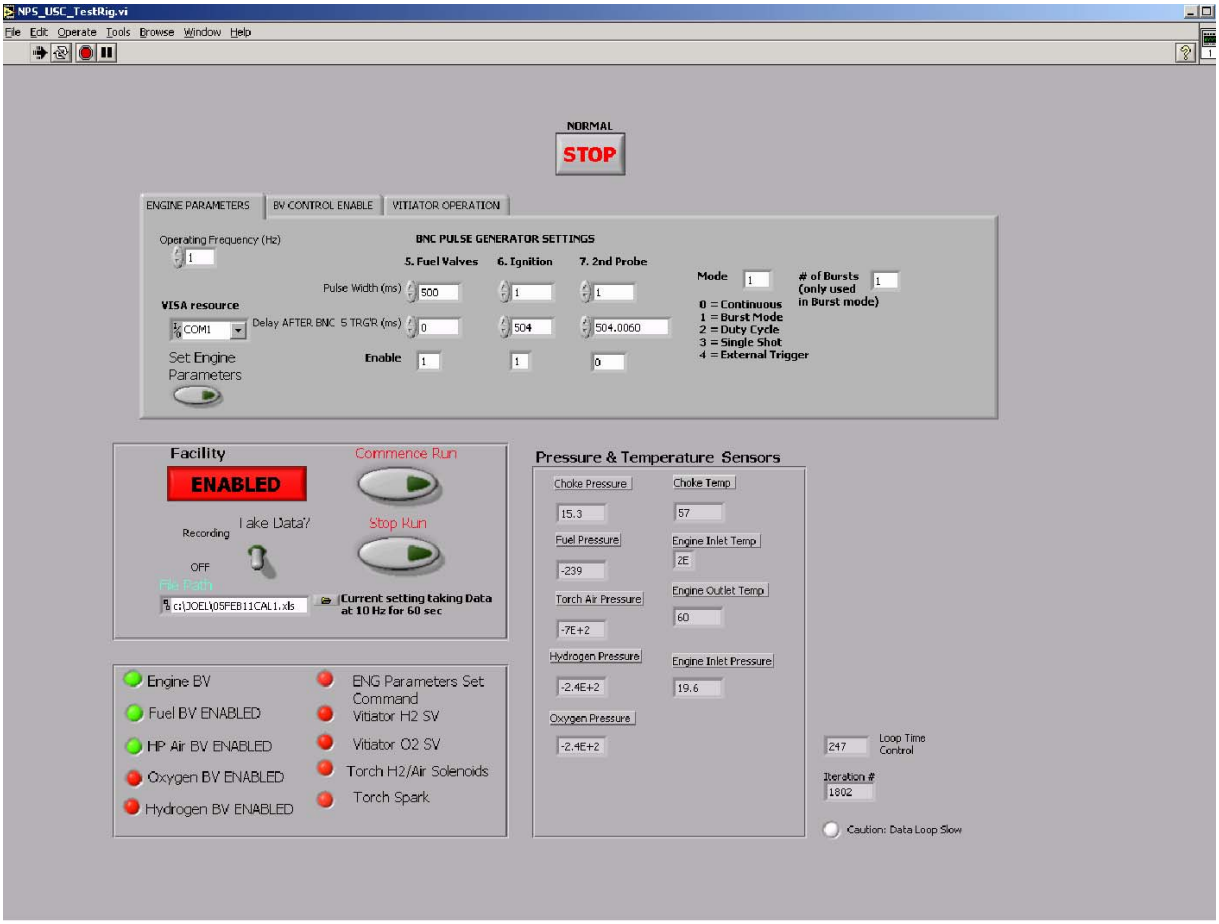

Figure 30. Test Cell One LABVIEW Front Panel View

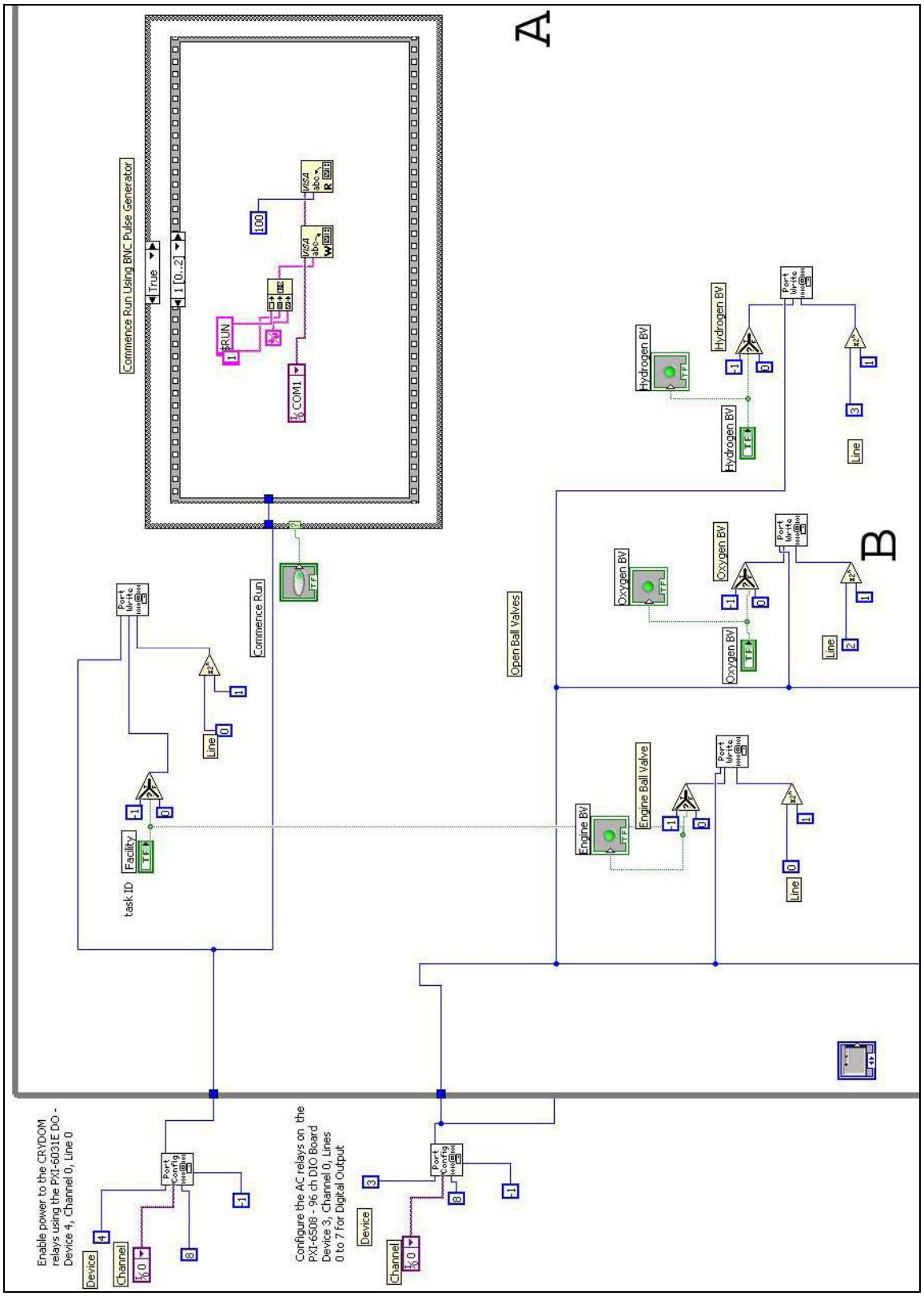

Figure 31. Test Cell One LABVIEW Code Screen 1

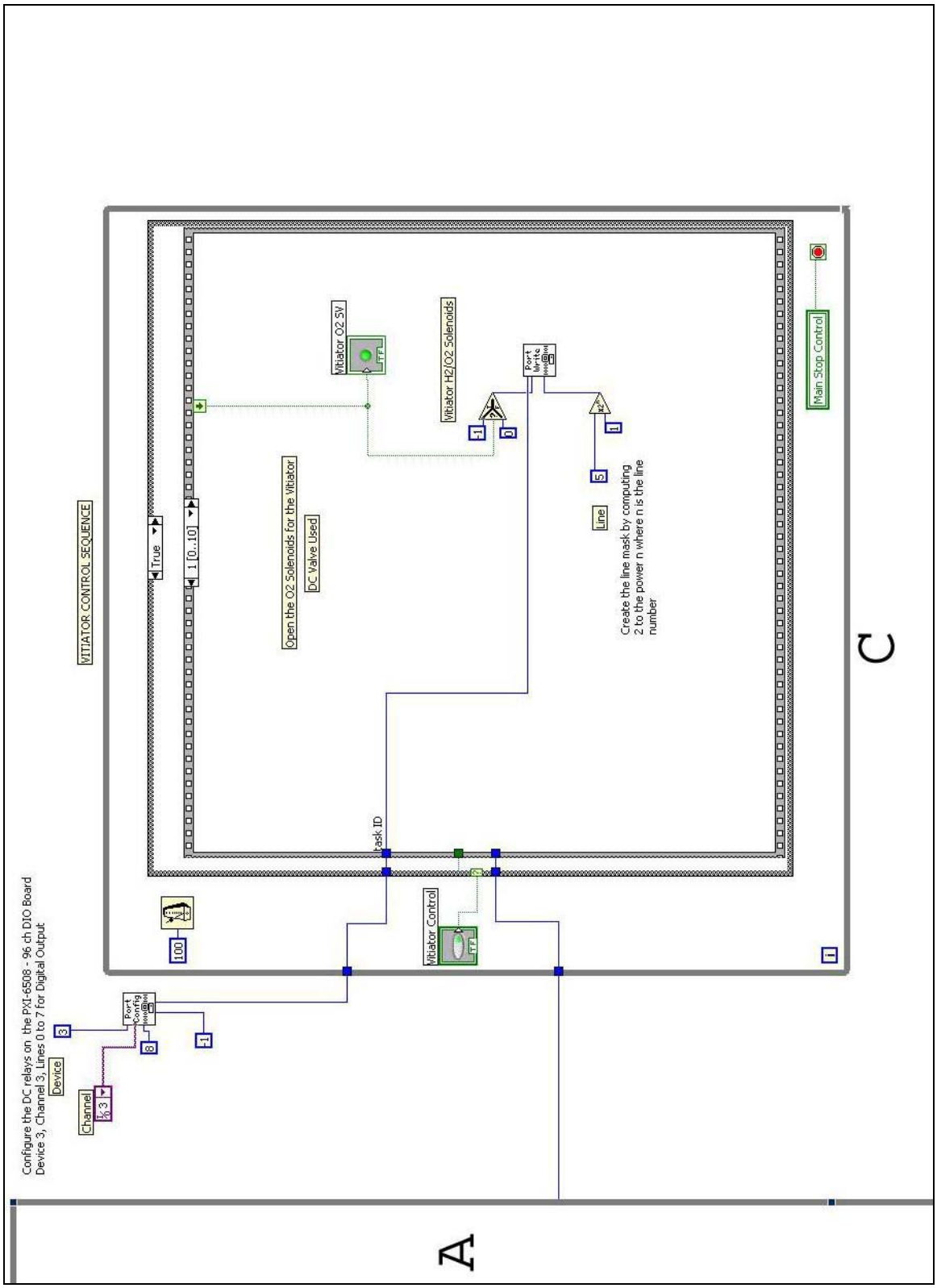

Figure 32. Test Cell One LABVIEW Code Screen 2

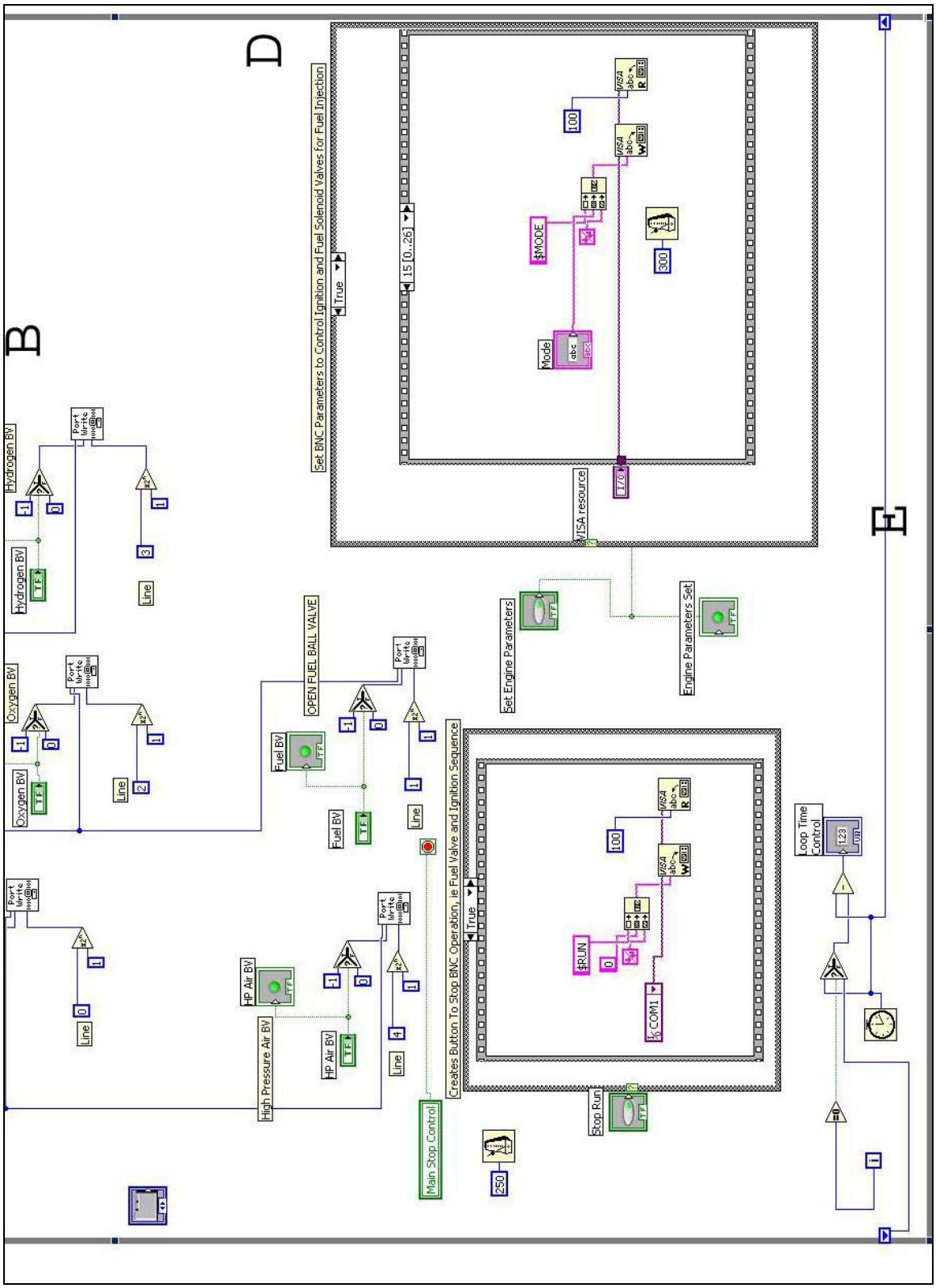

Figure 33. Test Cell One LABVIEW Code Screen 3

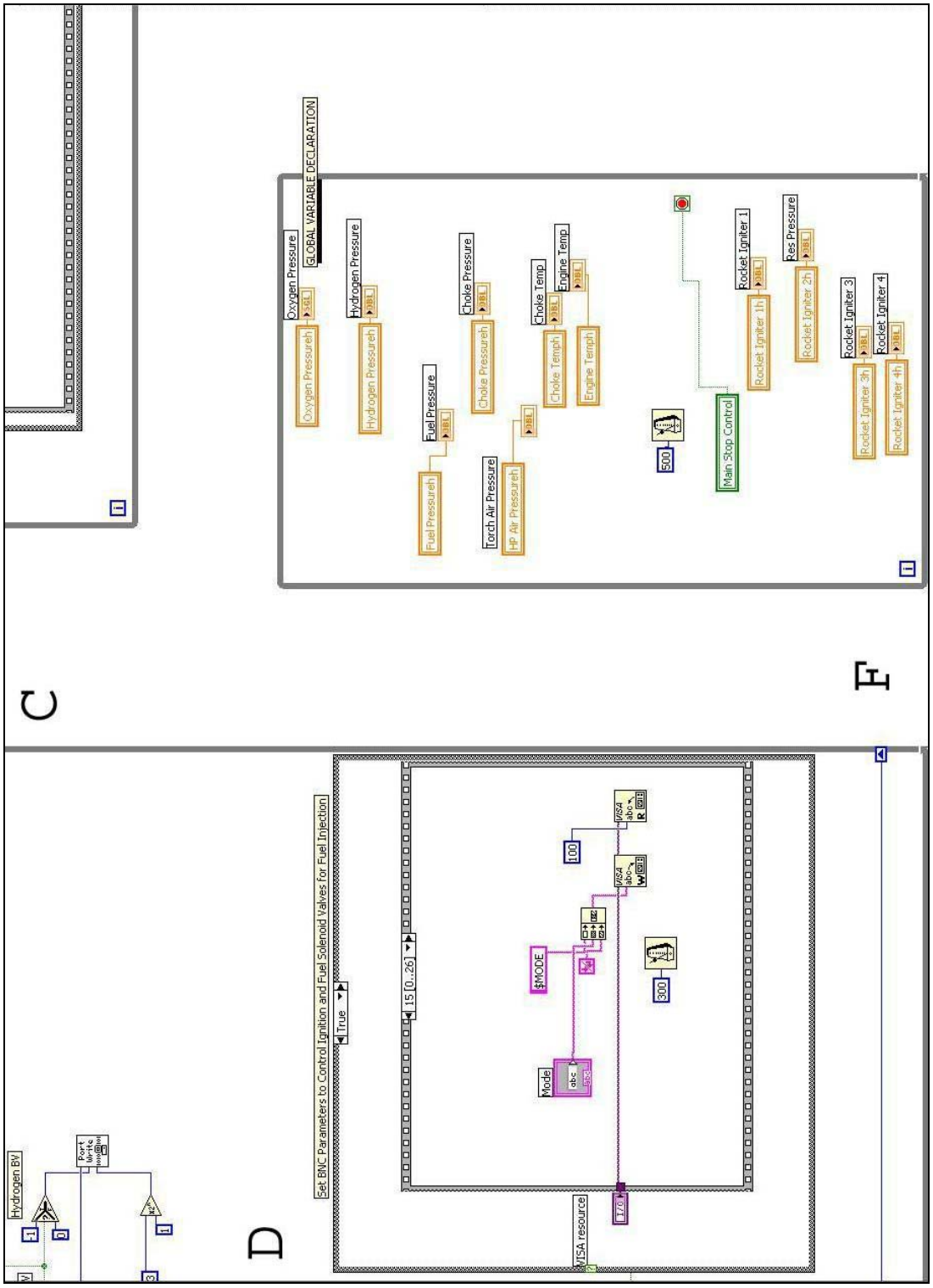

Figure 34. Test Cell One LABVIEW Code Screen 4

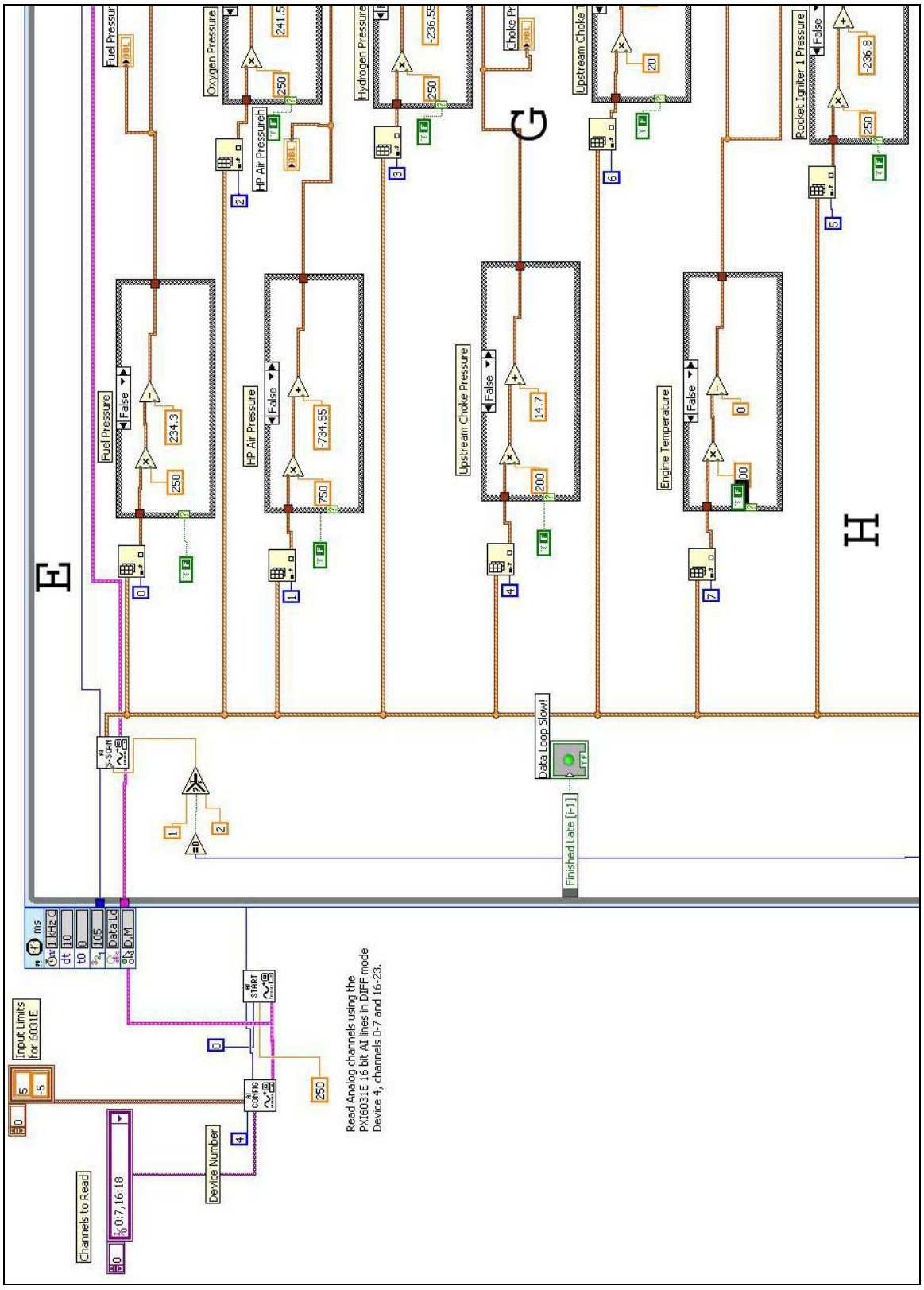

Figure 35. Test Cell One LABVIEW Code Screen 5

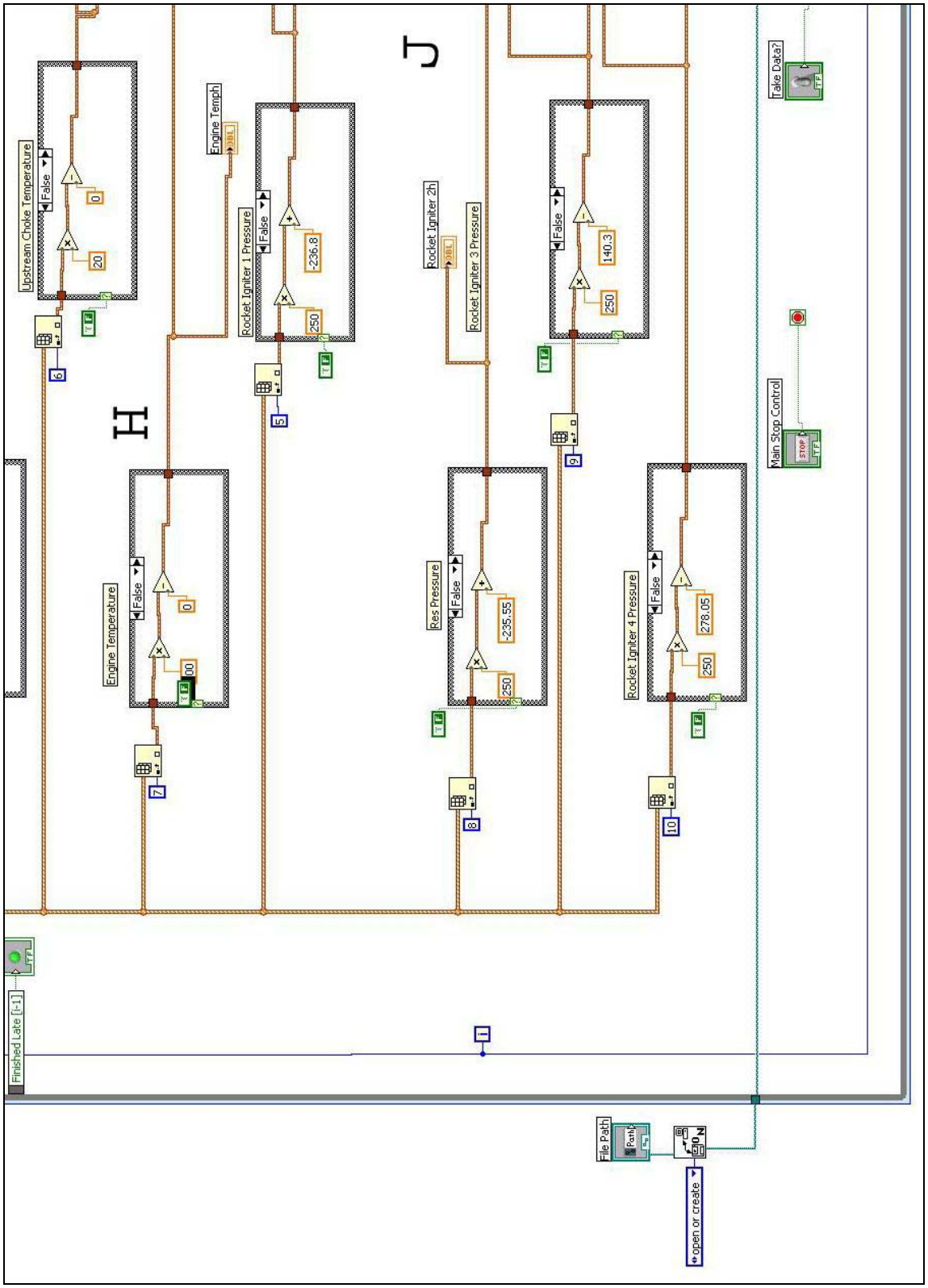

Figure 36. Test Cell One LABVIEW Code Screen 6

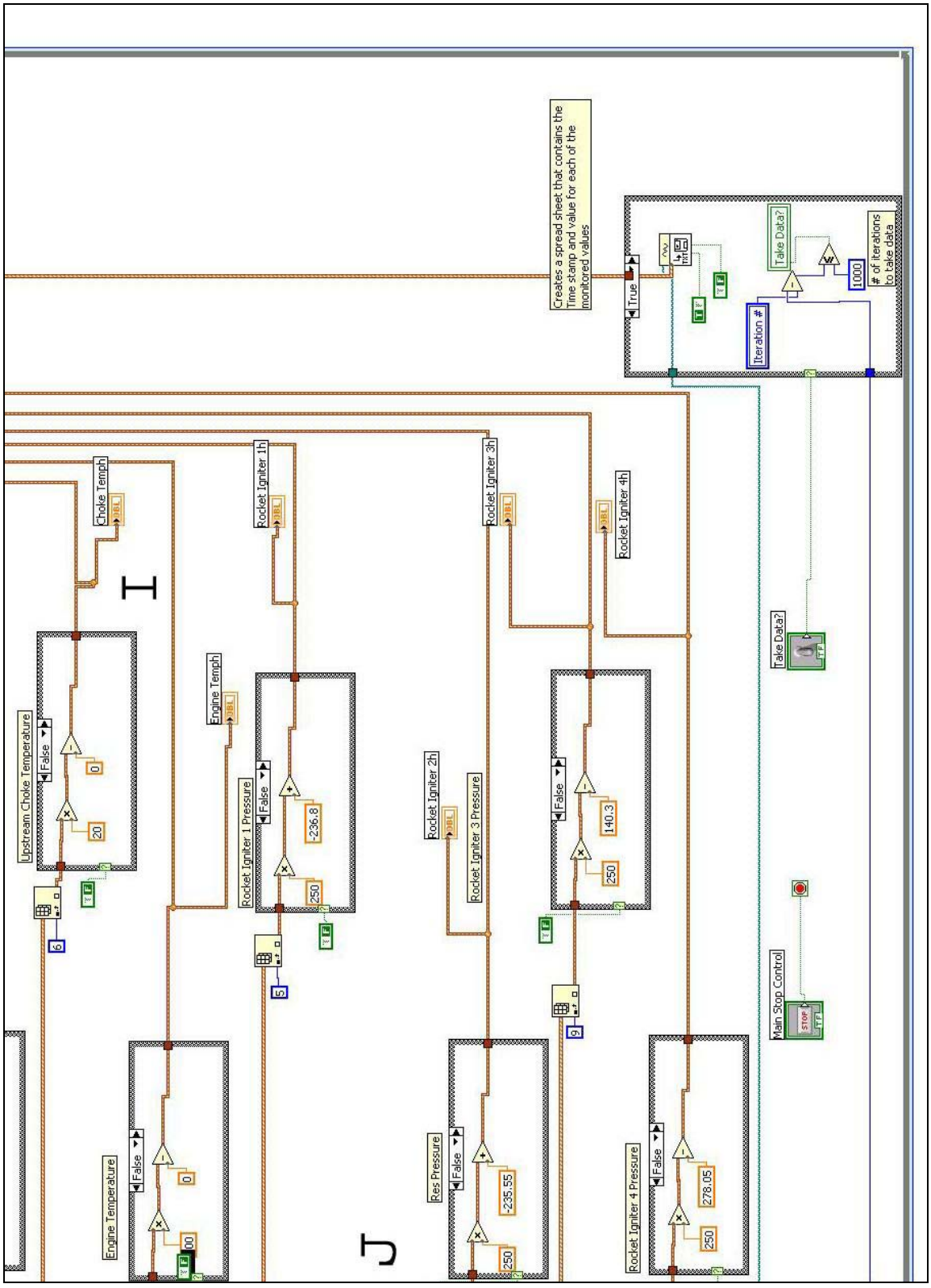

Figure 37. Test Cell One LABVIEW Code Screen 7

THIS PAGE INTENTIONALLY LEFT BLANK

APPENDIX C: CHIN SPIRAL SPECIFICATIONS

8380 Cerritos Ave
Phone (714) 995-5341 Fax (714) 995-7127

Spring Manufacturers Institute

Part Number	24 INCH COMPRESSION SPRING	Revision		Date	05/20/2004	Material	Music Wire		
Designer		Customer	US NAVY			Next Sm. Available		Next Lg.	Tensile
Wire Dia.	0.1250	Free Length	24.000	Works In		0.1200	No	0.1350	267120
Total Coils	10.000	Travel		Works Over		Units	English	Stress: Off	
Diameter	2.410 +-	0.125	D Type	ID	Max Solid				
					Dead Coils	G Mod	E Mod	Density	
						11500000	30000000	0.285000	
Condition	no preset, no peen					Spec.	ASTM A 228	APT	45
End Type	Closed -No Grind	Hand	Left						

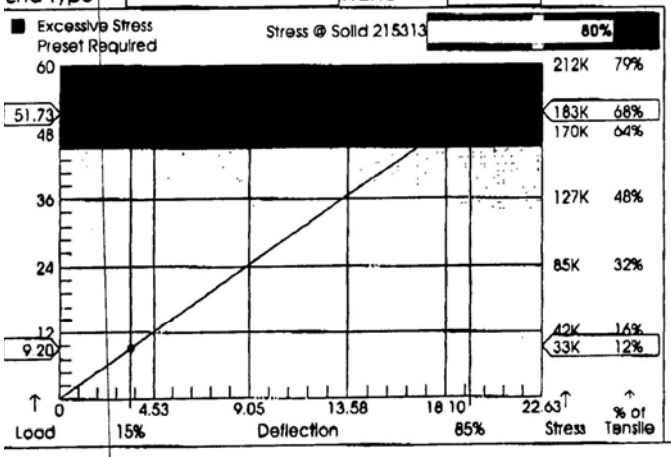

SpringRate	2.693	Pitch	2.953
Free Length	24.000	Pitch Angle	20.345
Solid Height	1.375	Wire Length	83.177
Active Coils	8.000	Weight	0.29091
Total Coils	10.000	(Length Tol)	
Min. ID	2.285	Nat. Freq.	33.716
Max. OD	2.785	Stress Ratio	
MMC OD	2.957	Buckle @	19.998
Index	20.280	Corr Stress	182801

Spring Diagnostics

-- May not be suitable for cyclic service --
* Large Index (>15)
* Excessive Pitch Angle
* Spring will Buckle

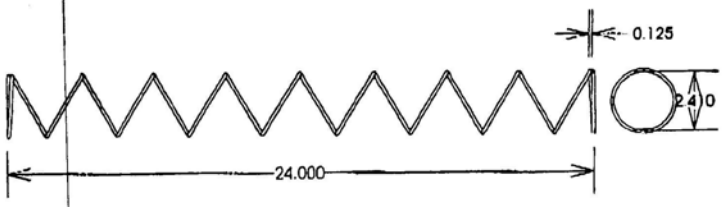

Drawing Notes

Compression -Dimensional

FAX 831 656-6201

TOTAL P.02

THIS PAGE INTENTIONALLY LEFT BLANK

APPENDIX D: TEST CELL #1 OPERATING PROCEDURES AND

Test Cell #1
Standard Operating Procedures (SOP)
(last modification date 14 Feb 04)

Safety Procedures

1. Notify all lab personnel of Test Cell operations, brief test plan.
2. Turn ON yellow caution warning lights (Surveillance Console)
3. Notify the Golf Course (x 2167) (Only required if Hot Fire Test is conducted)
4. Account for all personnel throughout Test Cell operations.

Preparing Test Cell

1. Boot up and configure SCARP, SAVAGE and PXI computers.
2. VERIFY Shop Air is and High Pressure Air is available
3. Verify CELL #1 Emergency Shutdown is PRESSED (secured) prior to entering test cell
4. ENERGIZE Omega Thermocouple Panels and Verify MSD Ignition DISARMED (CABINET #1A)
5. Turn ON 24 VDC and 110 VAC (CABINET #1A)
6. If required, set up any visual and or data recording equipment.
7. Enable test stand ignition system as required and connect 110 VAC vitiator power (if operating vitiator)
8. Turn on KISTLER amplifiers, specify and record scale settings, and set to OPERATE

9. Ensure that PXI Controllers and the 24 V DC switch (TESCOM Controller power) in Test Cell 2 in the black cabinets are ON.
10. OPEN Main Air Ball Valve diverting air to Test Cell 1, VERIFY Shop Air is open for Test Cell #1
11. OPEN Main Air (HP Air Tank Valve)
    a. Blue hand valve should be opened slowly as not to shock the lines
12. OPEN all applicable supply gas bottles
13. ENERGIZE Cabinet #2 (BNC)
14. Evacuate all non-essential personnel to the control room
15. On Scarp, open LABVIEW and ensure that the execution target contains the PXI address. Open control panel and run the program.
    b. RT Target address: 169.254.0.2
    c. Control Program Path
        i. Start \ Programs \ National Instruments \ LabView 7.0 \ LabView
        ii. Open \ RPCL \ JOEL\ LABVIEW \ NPS_USC_TestRig
        iii. Before running the vi, ensure that the name for the data file is changed so the previous file is not lost.
            1. Change name in file path box prior to running vi.
16. On Savage, open LABVIEW and ensure that the execution target contains the PXI data logger address. Open the control panel and start the High Speed Data Logger
    d. RT Target address: 131.120.20.112
    e. High Speed DAQ Path

i. desktop\4ch(digital trigger).vi

ii. Set the Trigger switch to EXTERNAL

iii. Start the program (the data logger will not start taking data until it is triggered by the Ignition trigger)

iv. Note: The Data logger does not stop automatically unless it completes its number of scans

Running the Combustor

1. Set All Engine Control Parameters (on BNC Pulse Generator)
    a. Send Engine Parameters to BNC
2. Set Main Air, Secondary/Purge Air, and all other gases pressures (ER3000) ON SAVAGE
    a. Set Main Air and Purge Air (ER3000)
        i. 001 Main Air (If running vitiator, wait until step 14)
        ii. 004 Secondary Air
    b. Supply Gases in Test Cell #1 TESCOM Node Address
        i. 002 O2
        ii. 003 Fuel
3. Set Hydrogen Pressure (Manually)
4. Twist CELL#1 Emergency Shutdown Button Clockwise (CELL#1is now live).
5. In LABVIEW, Enable Facility
6. Open Supply Gas Ball Valves (Fuel Ball Valve Must Be OPEN!!!)
7. Enable MSD Ignition switch (ARMED)

8. Verify Golf Course is clear
9. Sound the Siren
10. If Vitiator is not used, skip to step 19

Running the Vitiator

11. Set Vitiator Parameters (Run time, etc…)
12. Engage Main Air flow (Air will flow when pressure is set with ER3000)

**********WARNING**********

The next step will result in the commencement of the Vitiator run profile.

13. START Data Recording
14. START VITIATOR
    a. Vitiator sequence will run for the time set and then stop

15. STOP Data Recording (If running engine, stop following run)
16. Go to Step 19 if Running Engine
17. Secure Main Air Flow
18. In personnel are entering Test Cell, Push Emergency Stop Button **IN**

**********WARNING**********

The next step will result in the commencement of an engine run profile and ignition.

19. When area is clear, START record VCRs
20. COMMENCE RUN in Labview.
    a. High Speed DAQ will be triggered and the engine profile will commence
21. STOP RUN in Labview
    a. Pulse generation will be stopped.
    b. High Speed DAQ must be manually stopped on Savage
22. Secure MSD Ignition System (UNARMED)
23. Stop Main Air Flow
24. Stop Data Recording
25. If personnel are entering Test Cell, PUSH CELL#1 EMERGENCY SHUTDOWN

TEST CELL LINE MAPPING

Low Speed Read

1.	T – Upstream Choke	-	Device 4, Ch 6
2.	T – Engine Inlet	-	Device 4, Ch 7
3.	P – Upstream Choke	-	Device 4, Ch 4
4.	P – Fuel	-	Device 4, Ch 0
5.	P – High pressure Air (vitiator)	-	Device 4, Ch 1
6.	P – Oxygen	-	Device 4, Ch 2
7.	P – Hydrogen	-	Device 4, Ch 3
8.	T – Engine Outlet	-	Device 4, Ch 5

High Speed Read

1. S – BNC Trigger Register - HS Ch 1
2. P – Combustor Pressure Transducer 1 - HS Ch 2
3. P – Combustor Pressure Transducer 2 - HS Ch 3
4. P – Combustor Pressure Transducer 1 - HS Ch 4
5. P – Combustor Pressure Transducer 2 - HS Ch 5
6. P – Combustor Pressure Transducer 2 - HS Ch 6
7. P – Combustor Pressure Transducer 1 - HS Ch 7
8. P – Combustor Pressure Transducer 2 - HS Ch 8

Voltage Output

1. Enable Facility - Devise 4, Ch 0, LN 0
2. AC Main Air Ball Valve - Devise 3, Ch 0, LN 0
3. AC Fuel Ball Valve - Devise 3, Ch 0, LN 1
4. AC Oxygen Ball Valve - Devise 3, Ch 0, LN 2
5. AC Hydrogen Ball Valve - Devise 3, Ch 0, LN 3
6. AC High Pressure Air Ball Valve - Devise 3, Ch 0, LN 4
7. AC Solenoid Valve Torch Hydrogen - Devise 3, Ch 0, LN 5
   AC Solenoid Valve Torch Air
8. AC Spark For Torch - Devise 3, Ch 0, LN 6
9. AC Solenoid Valve Vit Hydrogen - Devise 3, Ch 0, LN 7
10. 24 V DC Ignition For MSD - Devise 3, Ch 3, LN 5
11. 24V DC Solenoid Valve Oxygen - Devise 3, Ch 3, LN 4

BNC Pulse Generator

1. Data Trigger - BNC Ch 5
2. MSD Ignition/TPI 1 - BNC Ch 6
3. TPI 2 - BNC Ch 6

INITIAL DISTRIBUTION LIST

1. Defense Technical Information Center
   Ft. Belvoir, Virginia

2. Dudley Knox Library
   Naval Postgraduate School
   Monterey, California

3. Joel Rodriguez
   331 Spring St #1
   Newport, RI

4. Jose O. Sinibaldi
   Department of Mechanical and Astronautical Engineering
   Monterey, CA

5. Christopher M. Brophy
   Department of Mechanical and Astronautical Engineering
   Monterey, CA

6. George Hageman
   Department of Mechanical and Astronautical Engineering
   Monterey, CA